

THAAD-Like High Altitude Theater Missile Defense: Strategic Defense Capability and Certain Countermeasures Analysis

He Yingbo, Qiu Yong

By incorporating the publicly available information about the Theater High Altitude Area Defense (THAAD) theater missile defense system and making some educated guesses about the unknown parameters of the system, we construct a computer model of a THAAD-like kill vehicle to simulate the endgame homing process. Using this model, we simulate endgame homing processes against incoming targets of different velocities, corresponding to theatre and strategic targets. We also simulate homing processes against certain types of countermeasures. The simulation results demonstrate that, given state-of-the-art technologies for infrared sensors, ground-based radars, and divert/attitude control thrusters, first, a THAAD-like defense would have nearly the same miss distance and kill probability against a strategic target as against a theater

Received 23 October 2002; accepted 19 July 2003.

This article is about the authors' personal findings and views based on public literatures, and does not necessarily reflect those of China Academy of Engineering Physics.

The authors would like to thank the Security Studies Program (SSP) at the Massachusetts Institute of Technology for providing research fellowships under the former W. Alton Jones Foundation. The authors would also like to thank Dr. George N. Lewis, associate director of the SSP and author of Appendix C, and professor Ted Postol for their suggestions and kind help in finishing this article.

Address correspondence to Qiu Yong, Massachusetts Institute of Technology, 292 Main Street, E38-658, Cambridge, MA 02139. E-mail: qiuyong@mit.edu

He Yingbo and Qiu Yong, Institute of Structural Mechanics, China Academy of Engineering Physics.

target, and second, countermeasures, like infrared stealth, radar jamming, and decoys, have the potential to defeat a THAAD-like kill vehicle using infrared homing during the endgame.

INTRODUCTION

The current Bush administration's missile defense program no longer distinguishes between strategic defense (former National Missile Defense, NMD) and theater missile defense (former TMDs). It is developing a so-called layered defense system to intercept a threat missile in all phases of its flight. Correspondingly, ballistic missile defense systems are classified according to the phase they operate in, not according to their target. The Bush administration also plans to use the former Navy Theater Wide (NTW) theater system for strategic defense and has classified the Theater High Altitude Area Defense (THAAD) theater system as a terminal system. All these steps are blurring the distinction between the theater and strategic defense concepts. Although this might seem only a question of terminology in the absence of the Anti-Ballistic Missile (ABM) Treaty, it is still important to understand the strategic capability of the upper-tier TMD systems.

Moreover, with this blurring, the U.S. strategic defense capability can no longer be simply measured by the number of its strategic interceptors as could be done under the prior practice of thinking of strategic and theater defense systems as totally different defense systems against different kinds of targets. Some high-altitude TMD systems have components that are very similar to those of a strategic defense system, and some even share external sensors (for example, the Defense Support Program (DSP) satellites and early warning radars, EWRs) with the former NMD system (now the Ground-Based Mid-course System, GBM). So, if their kill vehicles (KVs) are capable of intercepting a strategic target, this category of high altitude TMD systems could have some strategic capability. And then the capability of a U.S. strategic defense would not be simply determined by its planned GBM system, but also by the capabilities of these nominal TMD systems. Furthermore, with all the shared external sensors ready and the mobility of the strategic-capable TMD systems, it is likely that a limited strategic defense capability could be turned into a much larger capability on short notice, which could change the political implications of U.S. missile defense dramatically.

The capability of a missile defense is generally measured in terms of its footprint and kill probability against a given type of target. The footprint is the size and shape of the area that a defense can attempt to protect from being hit, and the kill probability is the probability that an intercept attempt will be

successful.¹ Work has been done on the footprints of U.S. high-altitude TMD systems such as the THAAD system and the NTW system.² As for the kill probability, however, there is no publicly available information, although there will certainly be some classified assessments made before a specific design is chosen for a system.³

The kill probability of high altitude TMD systems depends on several factors. During maneuvering flight in the endgame, generally, the time of flight (TOF), the measurement accuracy of the line of sight (LOS) angle between the interceptor and target, the aim point determination,⁴ and the KV's dynamic response to maneuver commands are the main factors affecting miss distance.⁵ In the context of comparing the kill probabilities against strategic and tactical targets, the closing velocity is the only parameter that presents an intrinsic difference, given a specific engagement geometry. However, some independent technical analysts have argued that a 25% increase in the closing velocity would not cause a sharp change in the kill probability. For example, in 1998, George Lewis and He Yingbo argued that, unless a TMD interceptor's capability against the theater warhead was already marginal, a 25% higher closing velocity would not be expected to seriously degrade the interceptor's kill probability, since it must be over-designed to counter the wide range of circumstances that will occur during intercept attempts against long-range theater missiles.⁶ This conclusion is supported by administration and contractor statements.⁷

This article began as an effort to assess the viability of the speed limit approach of the TMD Demarcation Agreement.⁸ While the U.S. withdrawal from the ABM Treaty has made that question moot, the more general question of the ability of upper-tier TMD systems to intercept strategic targets, and in particular the effects of the higher closing speeds involved in strategic intercepts, is still important for understanding the implications of the U.S. missile defense program. One goal of this article is to use an integrated model to assess how the closing velocity affects the kill probability in an endgame engagement. A second goal is to assess the effectiveness of countermeasures designed to defeat a KV's endgame homing. The analyses presented show that the closing velocity cannot alone effectively demarcate the dividing line between theater and strategic systems, and that some countermeasures could result in catastrophic failures in endgame intercept for the system parameters assumed here.

The kill probability is by no means technically easy to assess because the three dimensional, 6 degrees-of-freedom numerical simulations that are typically used to evaluate the statistical properties of miss distance distributions are very time-consuming. In addition, since some aspects of U.S. TMD programs are highly classified, it is impossible to acquire precise design parameters for a defense system, complicating the kill probability analysis even further. Even

without these restrictions, however, it would still be very difficult to simulate real engagement scenarios with high confidence.

However, here we are interested only in understanding the fundamental behavior of the kill probability in interceptor-missile engagements without going into all the engineering details. To do this, a simplified exoatmospheric engagement simulation has been conducted and will be discussed. The first section briefly describes the THAAD system and its operational characteristics. In the second section, a THAAD-like working model is created based on available information on the state-of-the-art performances of ground based radars (GBRs), infrared (IR) sensors, divert and attitude control system (DACS), and navigation devices. Informed estimates are made about some system parameters where no public information is available. In a simplified one-on-one engagement scenario, the miss distance and the kill probability are computed for several combinations of parameters. This analysis provides some insight into the currently achievable theoretical hit accuracy, and how it is affected by changing parameters such as the closing speed and countermeasures. The calculation results and their implications are then discussed in the concluding section.

It must be noted that this theoretical simulation does not presuppose or imply that a missile defense system, once engineered, would work in the real world as it is intended. The theoretical computation here does not establish the reliability and effectiveness of the real system in real circumstances involving unexpected occurrences. This is a very complex issue and involves many factors that no simple model can reliably account for. However, these should not prevent us from drawing general conclusions from relative data.

THAAD SYSTEM CHARACTERISTICS AND OPERATION⁹

The THAAD system was one of the core Ballistic Missile Defense Organization (BMDO) TMD programs. In the renamed Missile Defense Agency (MDA), it has been classified as a terminal defense system. The system is designed to engage a wide range of theater ballistic missile threats at long ranges and high altitudes (upper-endo- and exoatmospheric). It, as an upper-tier system, provides multiple intercept chances and expands the footprint of the defended area relative to lower-tier systems such as Patriot. The THAAD system is composed of a launcher, interceptor missile, the TMD GBR, and a Battle Management/Command, Control, Communications and Intelligence (BM/C³I) system. Table 1 summarizes the technical characteristics of its interceptor and radar in more detail based on the THAAD system as of the mid 1990s.¹⁰

Table 1: Brief technical characteristics of THAAD interceptor, KV and GBR.

Components	Descriptions
Interceptor	Single stage solid booster, burn time 17 seconds (s) with 2.7 kilometer per second (km/s) burnout velocity. KV mounted in front, total weight 600 kilogram (kg)
KV	Hit-To-Kill, separated from booster after burnout, cooled midwave InSb IR FPA, 256 × 256 pixel, uncooled window, liquid divert and altitude control system
GBR	X-band (~10 ¹⁰ Hertz), 9.2 m ² antenna

*For more interceptor and GBR parameters, see BMDO fact sheet 97-21 and Lisbeth Gronlund et al., "Highly Capable Theater Missile Defenses and the ABM Treaty," *Arms Control Today*, Vol. 24, No. 3, April 1994, 3-8. For the seeker parameters, see David Hughes, "U.S. prepares THAAD for Hit-to-Kill Test," *Aviation Weeks & Space Technology*, 30 October 1995, 25.

Before trying to model the THAAD KV, it is helpful to take a look at what a THAAD system deployed in the U.S. would do during a typical engagement against an incoming missile.¹¹ After a missile aimed at U.S. territory is launched, the following steps would occur:

1. After the missile breaks cloud cover but while its booster is still burning, it is detected and then tracked by DSP satellites or future Space-Based Infrared System (SBIRS) satellites in high earth orbit. Stereo DSP observations can give a preliminary state vector of the missile. If the low-altitude part of SBIRS, SBIRS-Low (formerly known as the Space and Missile Tracking System-SMTS), is deployed, it will be able to track missile targets even after their booster burns out. Depending on where the launch site is, immediately or after some time delay following booster burnout, the missile would also be detected and tracked by EWRs surrounding the United States in England, Greenland, Alaska, Massachusetts, and California, or by future missile defense radars. If THAAD were deployed on U.S. territory, the information obtained from these sensors would be relayed to the THAAD BM/C³I system. This cueing information would reduce the area in the sky that the THAAD radar needed to search and thus allow it to achieve a larger detection range. If SBIRS-Low satellites are deployed, their measurements would be accurate enough that detection of the target by the THAAD GBR is not necessary for the launch of an interceptor;
2. Based on the location and the known dynamics of the THAAD interceptor, coupled with the predicted future state of the attacking missile, a so-called Predicted Intercept Point (PIP), which is a calculated position in space where the target and interceptor could coincide, is generated by the THAAD BM/C³I. The PIP accuracy improves over time. Once the expected value of the PIP error falls below a threshold value, a launch solution in which an

interceptor can be guided to the PIP is formed and an interceptor is committed and launched. This required PIP accuracy should be such that the probability is high that the interceptor's maneuvering capability can remove any error;

3. After the launch of the interceptor, the THAAD radar tracks it and transmits guidance and navigation messages, allowing the booster to correct its course with thrust vector control during the boost phase. After its booster burns out, the KV separates and its midcourse fly-out begins. The KV receives several In-Flight Target Updates (IFTUs) from the GBR that provides updated, predict-ahead target position, time, and velocity for use within the KV's control suite to make mid-course corrections. The KV responds to the updates by maneuvering toward the updated PIP by firing its divert thrusters. The BM/C³I system uses the radar data to produce a "Target Object Map" (TOM) and to transmit it to the KV prior to the handover to the IR seeker. This TOM is a data set that contains position estimates for the target and for other objects predicted to be in the interceptor's field of view (FOV),¹² and is used in target designation.
4. When the KV reaches the predetermined handover point, the shroud is ejected and the attitude control thrusters fire to expose the IR seeker to the area in space where the target is expected to be. For the IR seeker to spot the target, the PIP must be accurate and the sensitivity and FOV of the seeker must be adequate.
5. The seeker acquires the target and identifies it by correlating the IR images to the TOM, or based on its own IR signature. The endgame in which the KV is on its own then starts. The integrated avionics package (IAP) filters the IR seeker data and the inertial measurement unit (IMU) measurements, uses the chosen navigation law and the aim point selection algorithm to compute the commands that will control the DACS thrusters and steer the KV into a collision course with the target.
6. Before the impact, the KV downlinks information that could help the BM/C³I make a kill assessment and that would be useful to subsequent THAAD interceptors. If it is decided that the intercept is a miss and that another THAAD intercept is impossible, then the BM/C³I passes the data to a lower-tier system.

THAAD KILL VEHICLE MASS MODEL

A very basic condition for hitting a target is that a KV's maneuver capability must be sufficient to remove the PIP error and allow it to reach the target.

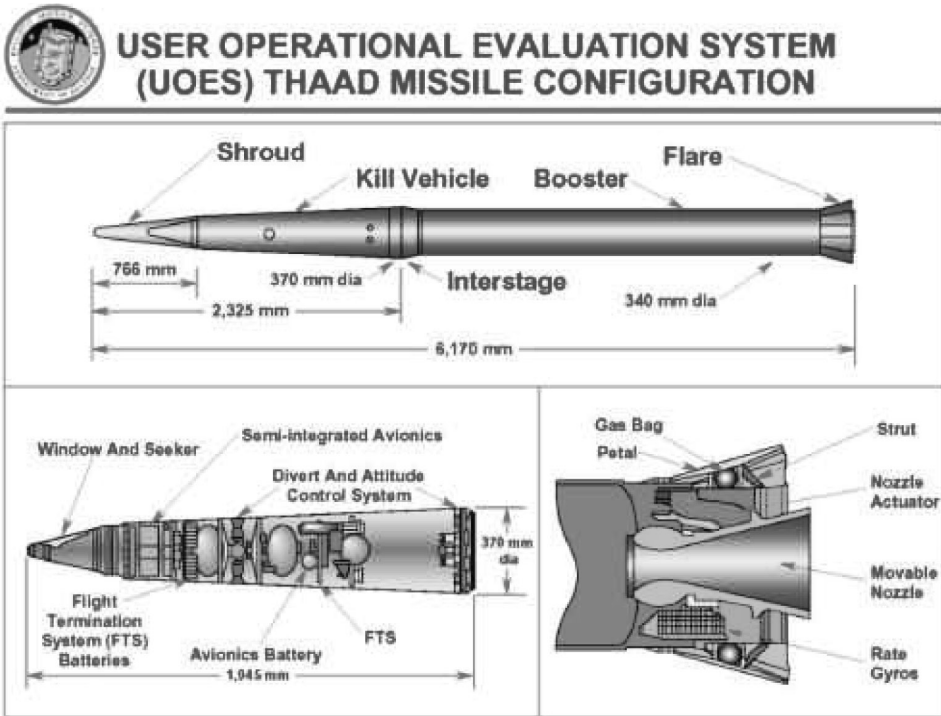


Figure 1: BMDO THAAD missile configuration. (User operational evaluation model.)

Because the amount of fuel carried by the KV, the KV's dry mass, and its time of flight (TOF) during the endgame are among the most important factors that determine the KV's maneuver capability, a THAAD KV mass model is needed for evaluating its performance. Interceptor size and weight limitations, which are related to system cost and transportation requirements, limit the amount of fuel available on the KV.

Although the KV's overall size is given in Figure 1, official data on its mass is not publicly available.¹³ In this section, by estimating the PIP accuracy and the KV divert system performance and by scaling the size of the fuel tank and the oxidizer tank, a KV mass model is deduced.

PIP Accuracy

The variation of the PIP accuracy over time is a very important consideration in designing a defense system since it can be traded off against the KV's divert

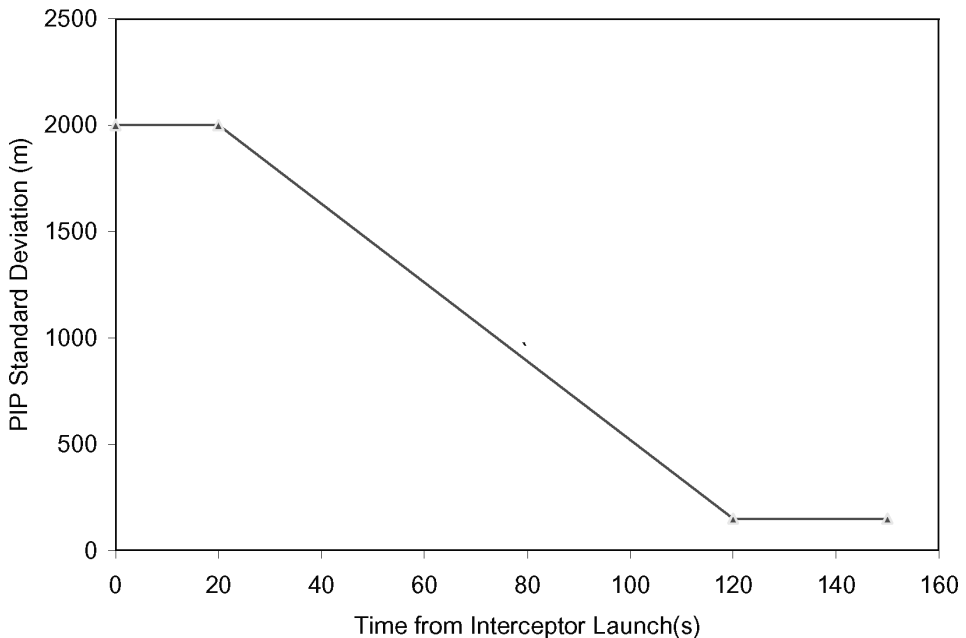


Figure 2: PIP errors assumption used in our analysis. By the time the interceptor is launched, the PIP error is assumed to be 2000 m; then it drops from 2000 m to 150 m. This assumption is based on our analysis on the tracking accuracy of external sensors and applies to both range and cross-range directions.

capability. Appendix A shows that in a THAAD-like engagement, the PIP error may be as large as 1.29 kilometer when the KV's midcourse flight starts, and as small as 80 m when endgame flight starts. To be conservative, we assume that the 1σ PIP error is 2.0 km from 0 second to 20 second (during this time interceptor is mostly in its boost phase), and it then decreases linearly with time to 150 m at 120 seconds, and remains so until 150 s (the beginning of the endgame). This simplified PIP error update timeline model is shown in Figure 2. This PIP variation applies to both cross-range and down-range directions.

Midcourse Maneuver Requirement

The PIP accuracy improves during the KV's midcourse flight, so updated PIP data is provided to the KV as it flies to the target. In our model, the KV's divert thrusters fire several times in order to place the KV into a "handover basket" with a 150 m diameter prior to the predicted time of target acquisition by the KV's IR seeker.¹⁴

Table 2: Divert requirements for 1σ error with two maneuvers.

Order of maneuvers	Time between maneuver and intercept	Maximum distance to be removed	Maximum divert velocity required
First	100 s	555 m	5.6 m/s
Second	30 s	1295 m	43.2 m/s

*The time needed to reach the divert velocity depends on the divert acceleration. It is very short for an acceleration of 3 g, and it is neglected in the article.

It is unclear to the authors how this improved PIP information is actually utilized by the divert system, but the general rule should be the sooner, the better, and the more frequent, the better. It has been reported that the DACS system might be fired six times in an actual situation.¹⁵ Table 2 shows that two such midcourse maneuvers, at 50 seconds and 120 seconds after the interceptor launch, would require 48.8 m/s divert velocity. If six such maneuvers are performed during KV's midcourse flight, starting at 35 s and ending at 110 s, once every 15 s, then only 24.4 m/s midcourse divert would be enough to do the job. A higher frequency of divert improves the maneuver effectiveness, but the improvement is not significant. Based on this analysis, it is reasonable to assume that a 100 m/s midcourse divert velocity would be able to provide 3σ confidence to remove a 1.85 km PIP error, leaving only a 0.3% probability of insufficient divert capability in one direction. We will see later that this 100 m/s midcourse divert, together with midcourse attitude control, consumes about 47% of the KV's overall fuel.

THAAD KV's Fuel

Now we estimate the amount of fuel that could be available to the KV during midcourse and endgame flight.

First, the fuel is assumed to be a combination of Monomethyl hydrazine (MMH) and Nitrogen tetroxide (N_2O_4), which is the dominant propellant combination for spacecraft propulsion. N_2O_4 ignites spontaneously on contact with MMH; therefore, igniters are not required. This property makes pulsing performance practical with storable propellants.

A fuel tank and an oxidizer tank can be clearly recognized in Figure 1. Both appear to be ellipsoidal and of same size. As Figure 1 is presumably drawn to scale, the approximate sizes of both tanks can then be obtained by scaling the size of the drawing. The three diameters of the tanks are measured to be 130 mm, 220 mm and 220 mm. The densities of MMH and N_2O_4 at 68°F are 0.8765 g/cm³ and 1.447 g/cm³, respectively, giving the total fuel and oxidizer mass of 7.7 kg.¹⁶

If both tanks are of the same size and fully filled, the mixture ratio (MR) is about 1.65 at 68°F. The bipropellant combination of $\text{N}_2\text{O}_4/\text{MMH}$ produces a maximum specific impulse (I_{sp}) of 336 s when the MR is at its optimum value of 2.19.¹⁶ Because of the uncertainties associated with the MR and the fact that the I_{sp} is about 80% of its theoretical value when the pulse width is less than 20 milliseconds, the average I_{sp} is assumed to be 270 s.¹⁷

It is assumed that 10% of the fuel is consumed for attitude control during both midcourse and endgame flight, and that 5% of fuel is unusable due to various reasons. If the total fuel used in midcourse, including the fuel for both divert and attitude control, is M_{mid} , then the fuel used for divert in midcourse is $0.9 \times M_{\text{mid}}$; and the fuel used to divert in one direction is $0.5 \times 0.9 \times M_{\text{mid}}$. In one direction, using the rocket equation to calculate the midcourse divert velocity, we have

$$\Delta V_1 = I_{\text{sp}} g \ln \left(\frac{M_{\text{KV}}}{M_{\text{KV}} - 0.5 \times 0.9 \times M_{\text{mid}}} \right), \quad (1)$$

where ΔV_1 is the midcourse divert requirement in this direction, M_{KV} is the KV's launch mass including the mass of dry KV, the shroud and the fuel, g is the acceleration of gravity and I_{sp} is the fuel's specific impulse.

The KV's launch mass is taken to be 44.5 kg (including 5 kg mass of shroud) from Theodore Postol's estimate based on the payload that the THAAD booster can deliver to a burn-out speed of 2.7 km/s.¹⁸ Then, by substituting $g = 10 \text{ m/s}^2$ and $I_{\text{sp}} = 270 \text{ s}$ into above equations, for $\Delta V_1 = 100 \text{ m/s}$ assumed in the preceding part, M_{mid} is calculated to be about 3.6 kg, of which 10% is used for attitude control and 90% is used for divert.

Therefore, 4.1 kg of fuel remains when endgame flight starts. According to our 5% unusable fuel assumption, the KV has about $M_{\text{end}} = 3.72 \text{ kg}$ fuel available for endgame divert and attitude control. If 90% of it is for divert, as we assumed before, then a total fuel of 3.35 kg can be used for divert in both directions; or 1.68 kg in each direction. Using the rocket equation, we estimate that this fuel can provide about 150 m/s of divert capability in each direction during endgame.¹⁹

KV's Thrust and Acceleration

The acceleration of our KV model is assumed to be 3 g by comparison to that of the LEAP KV in appendix B. Since the KV's mass at the beginning of the endgame is about 36 kg, a 3 g acceleration needs 1080 N of lateral divert force.²⁰ A 1080 N lateral force requires a fuel mass rate of 0.4 kg/s when

$I_{sp} = 270$ seconds.²¹ The 1.68 kg of fuel supply can sustain the continuous operation of one divert thruster for about 4.2 seconds. This 4.2 seconds of divert can remove a maximum distance of about 1.0 km in a 10-second period or 330 m in a 5-second period.

So far, a THAAD-like KV mass model has been developed. Our KV model has a total (endgame and midcourse) divert capability of about 500 m/s, comparable to the LEAP KV divert capability of 420–550 m/s in appendix B, but it is smaller than our 760 m/s estimate for the NMD kill vehicle. Moreover, the divert capability difference between the NMD KV and our THAAD-like KV is larger than it might appear since the longer detection range of NMD KV lets it achieve larger divert distances.

SIMPLIFIED ENDGAME SIMULATION MODEL

We now describe the endgame geometry and the basic assumptions made to simplify the simulation, and then discuss the simulation models for several key subsystems that are important for determining the miss distance.

Engagement Geometry

The engagement geometry at acquisition and some initial kinetic parameters are shown in Figure 3. The X-axis passes through the nominal KV position and the nominal target position.²² The Y-axis is perpendicular to the X-axis and the origin is at the center of the KV.²³

The nominal KV position is assumed to be accurate, and all errors are described relative to the KV. The deviation of the actual position from its nominal one is described in terms of its X and Y components, called the range error and the lateral position error respectively. They can be expressed by components of the cross-range error and range error of the THAAD GBR for a given geometry. If the target, the KV and the GBR were in line, then the KV's range error is the GBR's range error; and the KV's lateral position error is the GBR's cross range error. The deviation of the actual closing velocity from the nominal one is also described in terms of its X and Y components, called the range rate error and the relative lateral velocity error, respectively.²⁴ They are connected to the accuracy of the GBR's velocity estimates.

For a 50–100 km detection range, the kill vehicle travels at most about 15–30 km during endgame flight. Noting that the distance between the GBR and the PIP is about 270 km when the endgame starts, the KV can be up to 235–255 km away from the GBR when the endgame starts according to Appendix A,

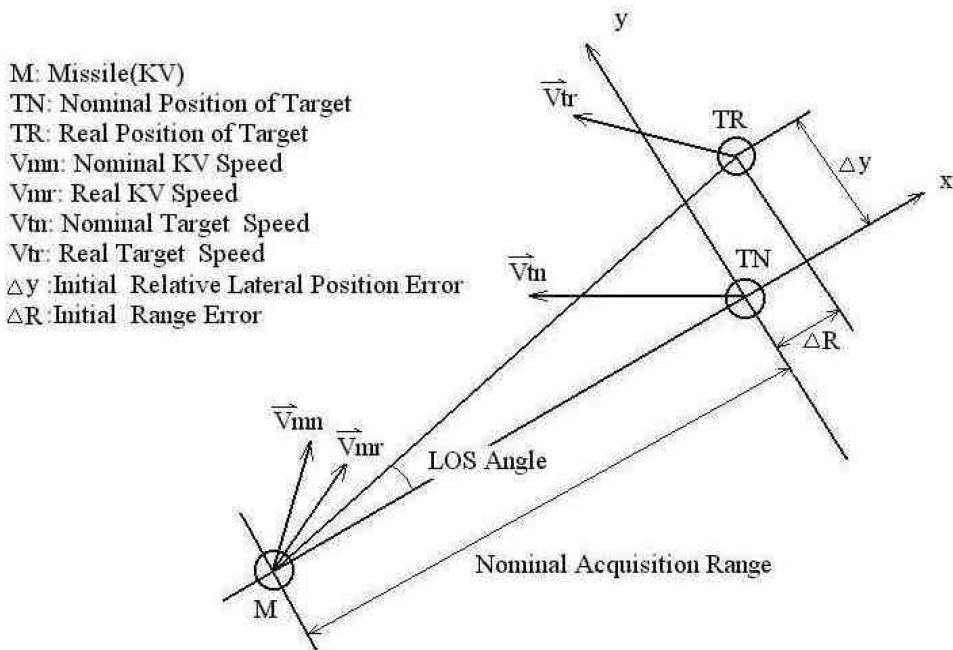


Figure 3: Endgame geometry used in modeling the endgame homing process.

indicating a initial lateral position error of about 25 m if the radar is on a line with the KV and target (using the angular tracking accuracy of 0.0001 radians in Appendix A). At the same time, the target is 290–330 km away from GBR, indicating a lateral position error of about 35 m. So when the BM/C³I passes the position information to the KV, the relative position error between KV and target is about 60 m at the beginning of endgame. Therefore, we assume a 1σ initial lateral relative error of 60 m.

Radar has a much higher measurement capability in the range direction. For a $S/N = 25$ and a 1 GHz bandwidth, the measurement accuracy in the range direction would be as small as about 1.5 cm.²⁵ However, if the KV’s LOS to the target is perpendicular to the GBR’s LOS to the KV, the KV’s range error could be the radar’s cross-range error. So we use the GBR’s cross-range measurement error as the KV’s range error, which is 60 m in this article.

It is not easy to estimate the GBR’s velocity measurement capability, in part because it also has range and cross-range components. Some points of comparison are available. One is Moshe Weiss’s estimate of the error in the

target impact velocity of 1.8 m/s obtained by filtering EWR tracking data (see Appendix A). The GBR's tracking accuracy should be at the same level if not better. Another velocity estimate is done by Theodore Postol, who estimates that the uncertainty in the radial component of a target's velocity as measured by the THAAD GBR is about 2.9 m/s.²⁶ To be very conservative, we assume the 1σ initial relative velocity error in both the cross-range and range directions are 10 m/s (as we will see later this relatively large value does not cause any problems).

For the endgame divert requirement, instead of the PIP error, it is clearer to use the so-called zero-effort miss distance (ZEM), which would be the miss distance if no corrections were made during the KV's endgame flight. The ZEM is the sum of the product of the initial relative lateral velocity and the TOF and the initial lateral position error. A 100 m ZEM error will result from the initial lateral velocity error of 10 m/s for 10 seconds endgame flight. Adding in the initial position error of 60 m, the ZEM is at most 160 meters. We assume the 1σ ZEM error is 150 m.

In summary, it is assumed that the 1σ initial range rate error and relative lateral velocity error are both 10 m/s (and have a Gaussian distribution). The 1σ initial relative lateral position error and the range error are both 60 m. And the 1σ ZEM error is 150 m.

Basic Assumptions

The following assumptions apply to our analysis:

1. The engagement takes place in the exoatmosphere so that there are neither aerodynamic forces nor aerooptical effects that degrade the performance of the IR seeker. The target travels at constant velocity. Because we consider an endgame that lasts only about 10 seconds, the effects of gravity can be neglected or dealt with by the guidance law. For the same reason, we do not deal with the Earth's curvature.
2. The model for KV-target kinetics assumes that the KV acceleration is normal to the initial nominal LOS, which we choose as X axis, and thus does not contribute to a change in the range rate.²⁷ The instantaneous range and range rate are estimated by the IAP based on the information provided by the GBR just prior to the target acquisition.
3. The KV is always correctly steered to the "handover basket" at the end of midcourse, so that the KV is in a position that allows it to see the target. The attitude control system works correctly so that the seeker can lock on to the target.

4. The KV's maneuvers in azimuth and elevation are decoupled. The amount of fuel consumed in the simulated direction is simply doubled to obtain the total fuel consumption; this is correct on the average, but will cause the KV to run out of fuel more often.
5. To simplify the calculation of the kill probability, the KV and the target are considered to be two spheres with the diameters of 0.5 m and 1 m respectively. This equivalently requires a center-to-center miss distance of less than 0.75 m for a successful intercept.

Seeker Subsystem

Even if the KV has enough endgame divert capability to remove the ZEM, other conditions must also be satisfied to hit the target successfully. One of these is that the KV's seeker should know the angular position of the target accurately.

The IR seeker senses the IR signal from a target. This signal is updated and transmitted to the IR image processor at a given frequency. The angular position of the target relative to the seeker's boresight axis is then obtained by locating the IR signal on the focal plane. This angle is added to the IMU's readout of the seeker's boresight angle to form the inertial LOS angle. The measurement accuracy, the data update frequency, and the acquisition range are three major specifications of a seeker subsystem.

The FOV and the number of pixels in the seeker's focal plane array (FPA) determine the measurement accuracy. The FOV, which is the angle subtended by the focal plane in one direction, is assumed to be 1 degree by referring to Appendix B. For exoatmospheric engagements and a focal plane with 256×256 pixels, or about 68 microradians (μrad) per pixel, it is reasonable to assume that:

1. The error of the off-boresight measurement from the IR seeker is less than one pixel, for three reasons. First, the image of a sphere with a diameter of 1 m occupies at most 2×2 pixels if the range is greater than 15 km; this condition is satisfied for at least 85% of the TOF for a 100 km acquisition range. Second, the image jitter due to aerooptical effects caused by the presence of air does not exist in the exoatmosphere. Third, a data processing algorithm can be used to obtain a subpixel accuracy when the image is larger than one pixel;
2. The error in aim point selection, which in this case is the distance between the aim point selected by the KV and the center of the target, is also within one pixel; and

3. Initial alignment biases affect the LOS angle measurements, but not the LOS rate, and the gyro drift and noise are the main error sources that affect the LOS rate. If the endgame lasts only 10s, the gyro's accuracy is $48 \mu\text{rad}$ for a gyro with one degree per hour class performance (see Appendix B), which is smaller than a one pixel accuracy of $68 \mu\text{rad}$.

Based on the above, it is assumed that the composite LOS measurement error due to seeker, IMU, and aim point selection errors is a uniformly distributed random noise parameterized by a half-width. Since each of these three errors is less than 1 pixel, the half-width of the noise, therefore, is assumed to be 3 pixels or about $204 \mu\text{rad}$. A uniformly distributed noise is worse than a Gaussian one from the point of view of the KV.

The seeker and the image processor are assumed to update data at a frequency of 50 Hertz (Hz).²⁸ This, then, is the frequency at which the navigation control computer issues the control commands for the DACS. The basic command period is then the reciprocal of that frequency, that is 20 ms. It is assumed that there is a delay time of 1 frame before the data from the image processor can be used by the navigation system. These specifications are not difficult to achieve given the current state of computer-related technology.

The acquisition range depends on the set-up of the seeker system (type of focal plane array, its sensitivity, size of the optical apparatus), background IR radiation, and the intensity of the IR signal from the target, which in turn depends on its size, surface coating and temperature. Appendix C estimates the minimum acquisition range of a THAAD-like kill vehicle, with a given set of parameters, to be at least 120 km.²⁹ The requirements on the acquisition range come from several considerations: (1) an early acquisition is desirable because the KV needs a sufficient number of target position measurements to get accurate enough estimates of target position; and (2) for a fixed closing velocity, a longer acquisition range will lead to a longer TOF, which in turn can either relax the system requirement on the ZEM due to its greater ability to remove a larger ZEM or lower the requirements on divert capability and fuel mass.

Kalman Filter

The KV's tracking accuracy is not simply the seeker's measurement accuracy. It improves as the number of measurements goes up because all measurement results go through an optimal digital noise filter, known as a Kalman filter.³⁰ We use a very simple two-state-variable Kalman filter to obtain an optimal estimation of the relative lateral position and velocity. The accuracy of a Kalman

filter depends on the following factors: (1) the accuracy of the description of the system dynamics (model imperfection); (2) the magnitude of the noise and the accuracy of the knowledge of the statistical properties of the measurements; and (3) the number of measurements.

The Kalman filter gives the best estimation of the LOS rate, which will then be used to calculate the desired acceleration through the proportional navigation law.

Navigation Law and Divert Performance

Once the Kalman filter provides an estimate on the target state, the navigation law is used to produce divert commands that will steer the KV correctly toward a hit, assuming the dynamic response of the divert thrusters is good enough to carry out the commands faithfully.

The KV is assumed to use proportional navigation, the law for which is of the form

$$n_c = N' \cdot V_c \cdot \dot{\lambda}, \quad (2)$$

in which n_c is the commanded acceleration normal to the LOS, N' is the effective navigation ratio, V_c is the closing velocity, and $\dot{\lambda}$ is the LOS rate. N' is chosen during the design of the navigation system, and is usually between 3 and 5; we choose 3 in this article. The value of V_c is the nominal value known to the defense and is transmitted to the KV prior to acquisition. The value of $\dot{\lambda}$ comes from the Kalman filter that filters the LOS measurements and computes the LOS rate.

The divert thrusters produce only one constant thrust level (either on or off) rather than a variable thrust, and the navigation system controls only their on-off pulse time. Thus, the control output should be on-off commands and pulse width information.

The performance of a thruster is characterized by its nominal thrust, thrust repetitiveness, and response time, which is the time needed for the thrust to rise from 0 to 90% of its nominal value. These parameters determine how fast and how accurately the KV can put itself on a collision course with the target if the control output is accurate. We have already assumed in the KV mass model that the thrust of a single thruster is 1080 N. According to test data of LEAP thrusters,³¹ the thrust repeatability averaged $\pm 10\%$ and $\pm 15\%$ for pulse widths longer and shorter than 20 ms, respectively and the response time was 5 ms for an “on” command and 3.8 ms for an “off” command.³² So it is reasonable to assume that the thrust repetitiveness of the THAAD KV thrusters is $\pm 15\%$ of

its nominal value (uniform distribution) and the response time is 5 ms to both on and off commands.

The divert thrusters are able to finely adjust the lateral distance. The minimum divert velocity bit is the product of the response time and the acceleration, which is 0.15 m/s for the THAAD KV. The minimum lateral distance bit within 20 ms can be as small as 3 mm, and this capability can be used to finely adjust the position of the KV when the time is very close to intercept so that it will hit a specific portion of the target.

If the estimated TOF is correct and the estimated relative lateral distance and velocity are also correct, the miss distance can be very small. Otherwise, the error in the Kalman filter's estimates of the lateral velocity along with the TOF error will also contribute to the final miss distance. It will be shown in the first simulation example that the Kalman filter can estimate the relative lateral velocity to an accuracy of 0.5 m/s under our assumptions.

Based on all the information and assumptions so far, a simplified numeric simulation program is created to simulate the KV's endgame flight, and the miss distance can be calculated when the initial conditions are specified in a single simulation. To get the statistical properties of the miss distance, the Monte Carlo method is adopted to calculate the kill probability. The random variables in consideration, which influence the miss distance, are: (1) the initial geometric and kinetic parameters at acquisition, which are randomly produced based on the statistical properties of the ZEM and the GBR capability (we assume that the accuracies of the ZEM and the GBR measurements are not affected by changing the target speed); (2) the seeker's measurements of the LOS angles relative to the actual LOS; and (3) the actual thrusts achieved relative to the nominal thrust.

SIMULATION EXAMPLES

In the following, we start with the simplest simulation, a single-run simulation where the defense system has accurate initial information about the range and closing velocity at the acquisition time. Then, we complicate the simulation by adding errors to the range and closing velocity. These single-run examples, of course, cannot be used to compute the kill probability, which is a statistical quantity, but help show how the simulation works and how capable the assumed KV is. In the case study section, we will assess the kill probability against theater and strategic targets, as well as certain countermeasures.

Single Run with Accurate Range and Closing Speed Information

Example 1. Theater Target with Range and Closing Velocity Known Accurately

In the first illustration, the KV flies at 2.7 km/s to engage head-on (crossing angle of 180 degrees) a theater target moving at 5 km/s. The initial range and the closing velocity are accurately known to the KV at the acquisition time, giving an accurate TOF estimate. The relative lateral position and the relative lateral velocity of the target provided for the KV at the acquisition time are 0 m and -20 m/s respectively while the actual relative lateral position and the actual relative lateral velocity of the target are 60 m and 10 m/s. The IR seeker acquisition range is 50 km.

The calculation results show that the final miss distance is -0.05 m, far less than 0.75 m, indicating a successful interception. The amount of fuel consumed was 3.36 kg, about 84% of the total endgame fuel.³³ In this case, the actual ZEM is about 120 m.

The curves in Figure 4 describe the histories of the actual relative lateral position and velocity and those estimated by the Kalman filter on-board the KV. They show that the KV can quickly correct the errors in its relative lateral position and velocity estimates. The estimated lateral position and velocity curves converge to the actual position and velocity curves after about two seconds are spent measuring the target position and correcting the KV's position. At the same time, the KV gradually aligns the closing velocity vector with the LOS by adjusting the relative lateral velocity. Thereafter, the KV is steered smoothly toward the interception point with little lateral divert because the KV is on the right course to hit the target if its LOS rate is zero.

Figure 5 gives a better understanding of how quickly the KV's estimation of the position and velocity is improved over the time and how accurate it is finally. This figure shows the actual lateral position error and the 1σ error of the KV's position estimation, as well as the same information for the lateral velocity. It is found that by the last 0.5 seconds the position and velocity accuracy of the Kalman filter has reached 0.25 m and 0.5 m/s, respectively. By that time, the KV has taken about 300 measurements (6 seconds, 50 Hz). The accuracies of the lateral position and velocity estimates just prior to intercept are better than 0.015 m and 0.25 m/s, respectively.

The dynamic response of the divert thrusters to divert commands is quick, and the minimum distance adjustment bit of these thrusters is also fine, leading to the very small miss distance. This result shows that the combination of the assumed performances of the sensor system and the divert system are capable of engaging theater missile targets, at least in terms of endgame performance.

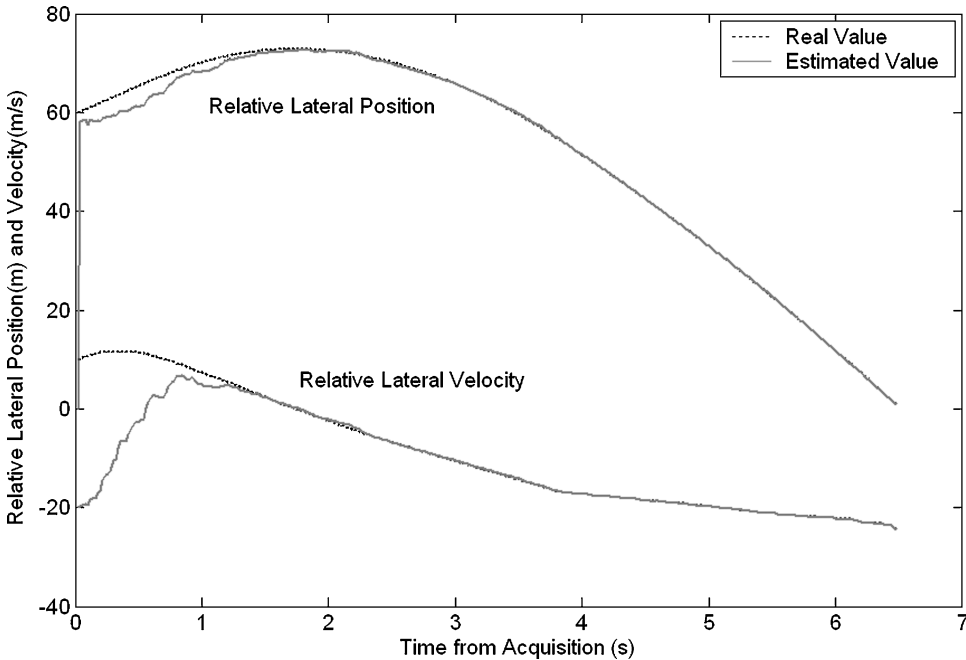


Figure 4: Relative lateral position and velocity history for Example 1. The relative lateral position and the relative lateral velocity of the 5 km/s target provided for the KV at the acquisition time are 0 m and -20 m/s, respectively while the actual relative lateral position and the actual relative lateral velocity of the target are 60 m and 10 m/s. The maneuver ensures the relative lateral position errors drop to almost zero and lead to a hit. The figure shows the miss distance is only -0.05 m.

Example 2. Strategic Target with Range and Closing Velocity Known Accurately

All the parameters are same as those in Example 1 except that the target is a strategic target with a velocity of 7 km/s.

The calculation results, some of which are shown in Figure 6, show that the final miss distance is -0.007 m, a figure not significantly different from that in Example 1. The simulation also shows that 3.33 kg, about 83% of the total endgame fuel, is consumed to remove a 110 m ZEM in the engagement. The accuracies of lateral position and velocity estimates just prior to intercept are better than 0.025 m and 0.25 m/s, respectively.

Although the target speed increases from 5 km/s to 7 km/s, the capability of the KV to engage the target does not appear to degrade to any significant degree.

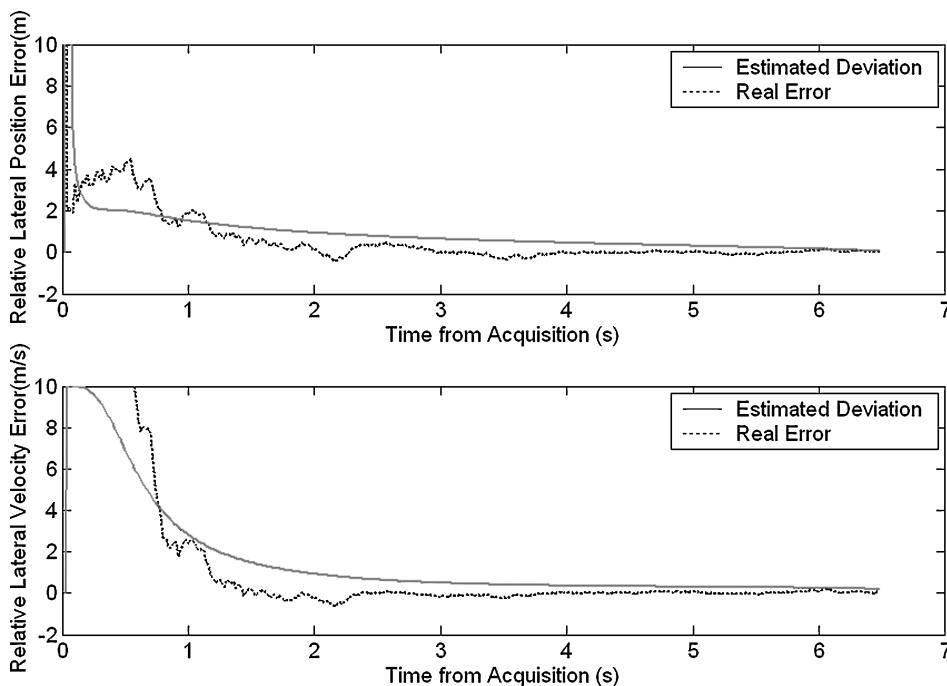


Figure 5: Actual and estimated relative lateral position and velocity errors for Example 1. The figure shows the target's relative position and velocity estimation errors of the KV drop as the number of measurements increases. The estimation accuracy reaches 0.25 m and 0.5 m/s, respectively, by the last 0.5 s.

Example 3. Strategic Target with Range and Closing Velocity Known Accurately, but Doubled Acquisition Range

All parameters are the same as those in the above strategic target simulation, except that the acquisition range is doubled to 100 km. The simulation produces a final miss distance of 0.05 m, and the fuel consumption is 3.64 kg for this successful interception. The accuracy of lateral position and velocity estimates just prior to intercept are better than 0.05 m and 0.25 m/s respectively.

Doubling the acquisition range does not enhance the performance appreciably because: (1) the seeker frequency is already high enough to guarantee that there are enough measurements to accurately locate the target even when the time available is only 5 seconds; and (2) given the same angular measurement noise, the shorter the range, the smaller is the 1σ cross-range position error based on a single measurement, giving a larger weight to the last measurements.

However, the longer TOF can allow the KV to remove a larger initial error or decrease the required amount of fuel in the design phase. However, in this

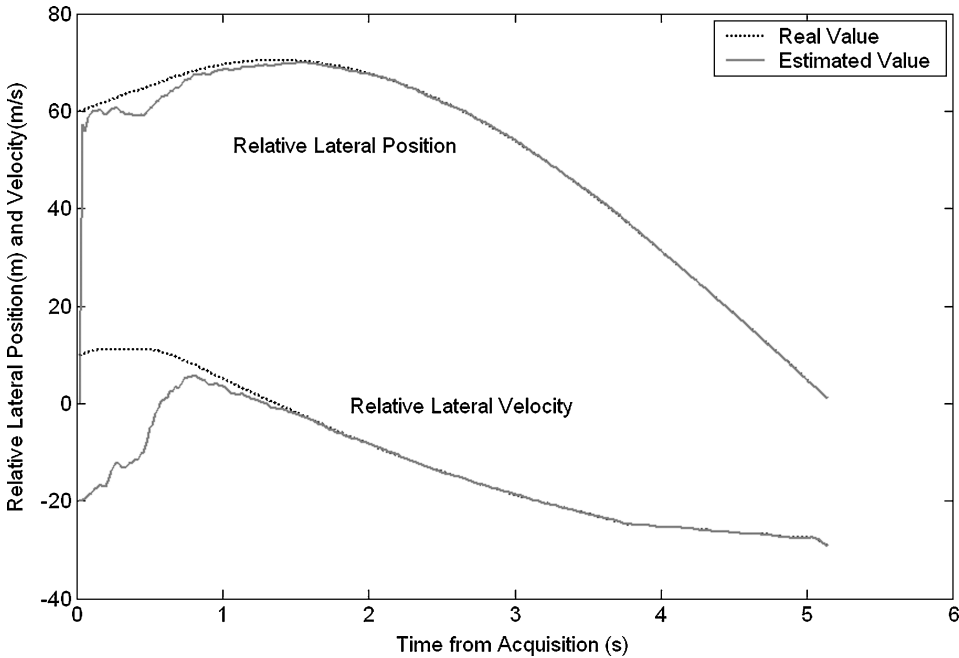


Figure 6: Actual and estimated relative lateral position and velocity error for Example 2. The relative lateral position and the relative lateral velocity of the 7 km/s target provided for the KV at the acquisition time are 0 m and -20 m/s, respectively, while the actual relative lateral position and the actual relative lateral velocity of the target are 60 m and 10 m/s. The figure shows the miss distance is only -0.007 m although the target velocity has been increased to 7 km/s.

case, where the ZEM is not very large (about 160 m), the fuel saving effect of a longer TOF is neutralized by the fuel spent in the second half of the TOF making tiny position adjustments.

Figure 7 summarizes the above three examples. It shows that, with the assumed performances of the seeker system and the divert system, the THAAD KV can achieve nearly the same final miss distance against a faster strategic target as against a theater missile target at either 50 km or 100 km acquisition range.

Single Run with Inaccurate Range and Closing Speed Information

In reality, the range and closing velocity is measured by the GBR and is updated to the KV before acquisition. This data cannot be 100% accurate due to

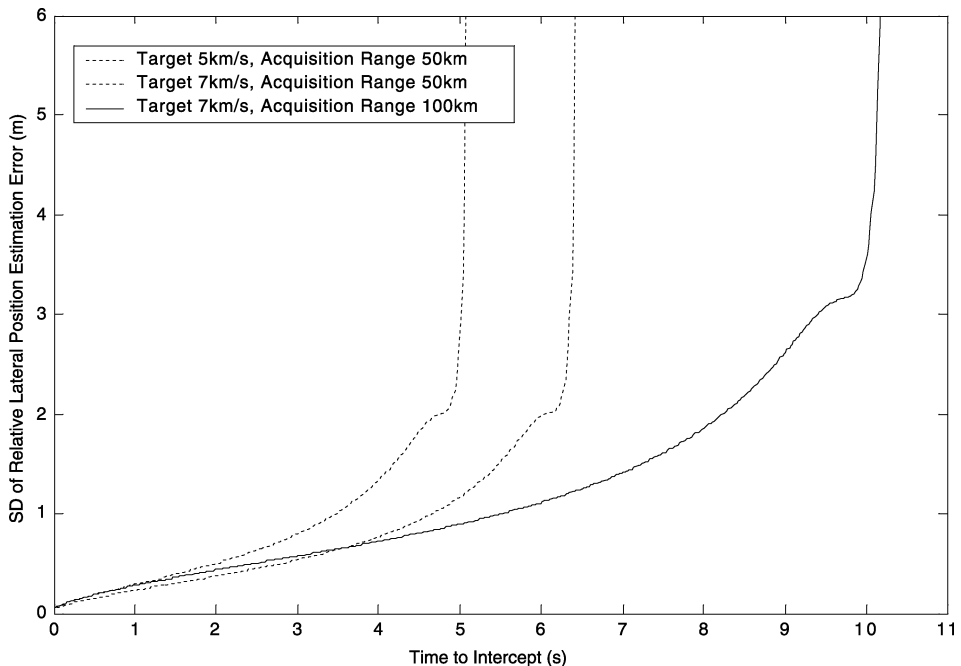


Figure 7: Comparison of one SD of estimated position for three examples. The figure shows the THAAD KV can achieve nearly the same final miss distance against a faster strategic target as against a theater missile target at either 50 km or 100 km acquisition range.

measurement noise. In addition to the errors in the initial lateral position and velocity estimates, the noise results in an inaccuracy in the TOF estimation, the effects of which will be considered in the following examples.

Example 4. Strategic Target with 100 km Nominal Acquisition Range

All parameters are same as those in Example 3, except that: in Situation 1, the actual acquisition range is 500 m less than 100 km, and the actual closing speed is 30 m/s larger than 9.7 km/s (thus, the nominal TOF is 10.3 seconds, about 0.1 second longer than the actual TOF of 10.2 s); and in Situation 2, the actual acquisition range is 500 m more than 100 km, and the actual closing speed is 30 m/s smaller than 9.7 km/s. (thus, the nominal TOF is 10.3 seconds, about 0.1 second shorter than the actual TOF of 10.4 seconds).

These two situations are chosen to maximize the error of the TOF estimation. A large range error of 500 m and a large velocity error of 30 m/s are chosen because they may represent the GBR's performance under some

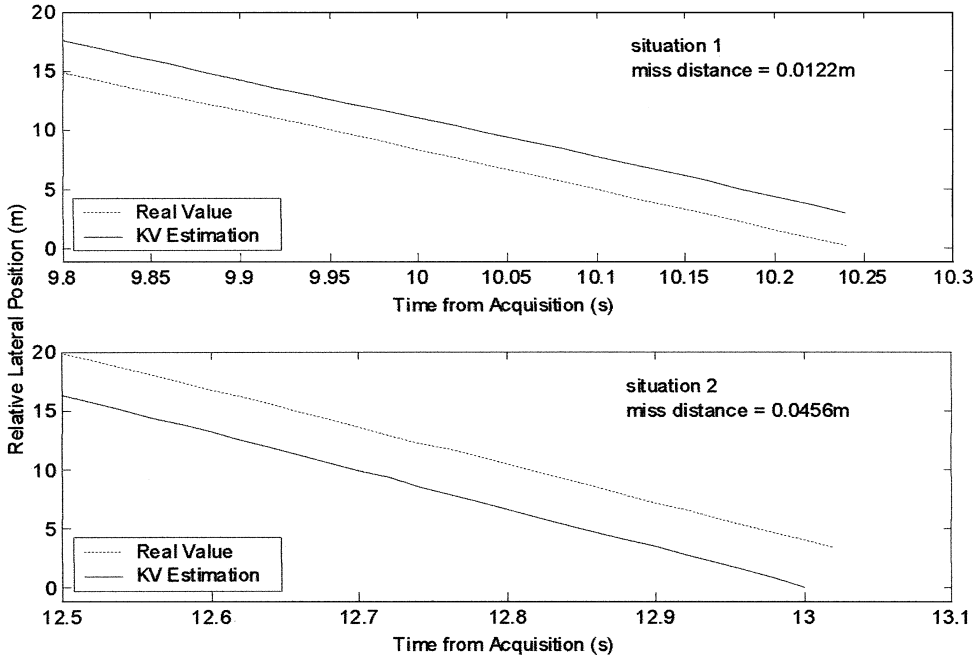


Figure 8: Actual and estimated relative lateral position when there is a 0.06 s TOF error. The figure shows the KV actually hit the target sometime earlier or later than expected because of the TOF error. This suggests that the hit is not sensitive to range and closing velocity error.

electronic countermeasures that degrade the radar performance but do not lead to large ZEM error.

In Situation 1, the calculation results show that the final miss distance is 0.012 m. From Figure 8, we can see that the KV actually hits the target about 0.06 seconds earlier than expected, and that the KV estimates that the target and the KV are about 3 m apart laterally at that time. The accuracies of the lateral position and velocity estimates just prior to intercept are better than 0.15 m and 0.25 m/s respectively. In Situation 2, the final miss distance is 0.05 m. The KV hits the target 0.06 seconds later than expected. In this model, the divert system does nothing after the moment at which it is expected to collide with the target because the KV's estimation of the time from interception is already zero. The errors of the last lateral position and velocity estimates prior to intercept are better than 0.06 m and 0.25 m/s respectively.

The explanation for the insensitivity of the miss distance to range error and closing velocity errors is that proportional navigation adjusts the velocity

vector of the KV to align the closing velocity vector with the LOS by using only angular rate information. Once it is on the right course, it will hit the target sooner or later because the velocity vector of the target does not change, at least for exoatmospheric intercepts. Although there is a velocity error of 0.3 m/s, it contributes only 0.02 m to the final miss distance, and this does not degrade the performance significantly.

The calculation results indicate that the endgame performance is not very sensitive to certain types of countermeasures against the GBR since a range error of 500 m and a velocity error of 30 m/s are severe performance degradations to the GBR. Thus, the KV design is quite robust against such inaccurate initial conditions updated to the KV at acquisition.

We have to note that, besides degrading the range and closing velocity accuracies, certain countermeasures against GBRs, such as radar jamming, could also degrade the accuracies of PIP estimates and other handover information. This implies that greater initial errors have to be removed and a larger ZEM error could occur, which could lead to a larger possibility of running out of fuel for KV. Moreover, the jamming could, to some extent, affect the GBR's capability to distinguish a warhead from its accompanying objects, especially decoys. We will discuss large ZEM caused by radar jamming later in this article.

Case Studies

Case 1. What Role Can a Theater Missile Defense Play on Current Strategic Defense?

The only intrinsic difference between a strategic target and a theater target in an endgame intercept for a given geometry is closing velocity, although there can be other differences between these two categories of targets. For instance, the strategic target is in general a small reentry vehicle (RV), while a theater target could be larger and could even be a warhead with a boost stage attached. So a theater target might be a stronger IR source due to a larger IR emission surface. This is true on average. However, in actuality, making this distinction could be difficult because there are significant variations among both strategic targets and theater targets. For example, a Russian advanced RV could be very different in size from a third country's rudimentary nuclear RV, or a Chinese RV. Furthermore, targets of the same size could have IR signal intensities that vary by factors of two or three or more due to temperature, surface materials of different emissivity, and differences in reflected sunshine and earthshine. The

orientation of the warhead could also cause variation of IR signal intensities. A defense system must be designed to deal with the variations that occur in real world situations. So IR signal differences based on targets' physical sizes are not necessarily distinguishing differences for the KV. Thus, the closing speed is the only intrinsic difference during the endgame intercept. However, in our consideration of possible countermeasures we will show how variations in IR signal affect the kill probability.

In the preceding section, the KV's miss distance has been shown to be not significantly different between theater and strategic targets. In this section, Monte Carlo simulations are carried out to estimate the kill probability against theater and strategic targets. The target speeds range from 5.0 km/s to 7.0 km/s with an increment of 0.1 km/s, and 1000 Monte Carlo runs are made for each increment.

The nominal acquisition range is 100 km. The 1σ ZEM is set to 150 m. The 1σ errors of the GBR's estimations of lateral position and range are 60 m. The 1σ errors of the GBR's estimations of lateral velocity and closing velocity are 10 m/s. Other unspecified variables are assigned the same values as in the single run cases.

The result in Figure 9 shows that the kill probabilities against different speeds are 99.8%–100%, all near 100%. The kill probability does not drop when the target velocity increases. This result suggests that a high-speed target does not pose a challenge to our model. By further examining all the failed trials, we find that all the misses are caused by lack of fuel, or exactly by the fact that the range error, lateral position error, and/or ZEM error, are larger than the KV's diverting capability can deal with in the TOF. A few such large errors are a normal phenomenon in a Gaussian distribution Monte Carlo simulation. So, it can be concluded that, assuming the system does not malfunction, for one-on-one engagements under our assumptions for the performances of the seeker, the Kalman filter, the DACS system, and the endgame guidance, the KV will always hit the target if the position and velocity errors are within the KV's diverting capability. Thus, the difference between the KV's kill probability against a theater target and a strategic target lies only in the difference of diverting capability due to the difference of TOF. But since the KV's acquisition range is large enough to provide enough maneuver time, the reduction of time due to a higher closing velocity does not challenge the KV's maneuver capability. So the kill probabilities in these two cases are the same. Another conclusion we can draw from Figure 9 is that out-of-fuel does not necessarily mean a miss of the target. This is because our simulation attempts to achieve a zero miss distance. So, even if it runs out of fuel, the KV may have already adjusted its trajectory accurately enough to hit the target.

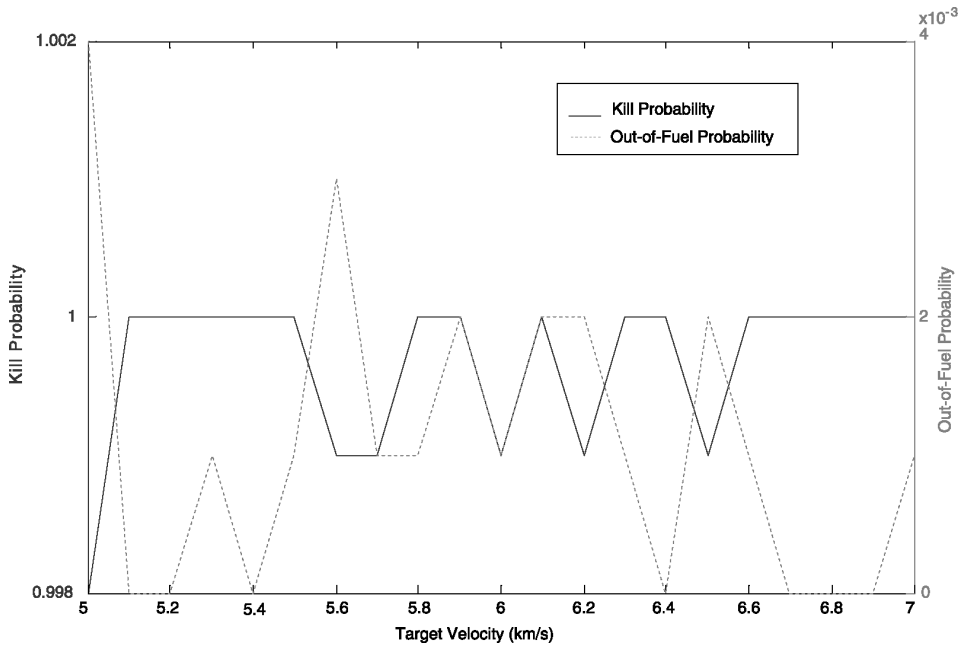


Figure 9: Kill probability and out-of-fuel probability vs. target velocity (note the right axis for out-of-fuel probability is in the order of 10^{-3}). The figure shows the kill probability remains almost 100% as the closing velocity increases from 5 km/s to 7 km/s. It also shows running out of fuel does not necessarily mean missing the target.

In a theater situation, there may not be accurate PIP information available until the THAAD radar begins tracking targets. To have a high kill probability in this situation, the THAAD can wait until its radar finds the target before launching an interceptor, resulting in a small footprint. This implies that the footprint can be traded off against the kill probability. Or it can use cueing information from future SBIRS-low-like satellite, or it can deploy radars forward. In this case, the theater defense system could have a good strategic defense capability with the help of external sensors.

Case 2. Effects of Certain Countermeasures

The effectiveness of a defense system is determined by many factors. An important factor is the possibility of countermeasures, which are steps the attacker takes to defeat the defense. In the *Countermeasures* technical report released in April 2000 by Union of Concerned Scientists and MIT Security Studies

Program, several countermeasures are assessed as potential threats to the effectiveness of the Clinton ground-based NMD program.³⁴ That report contains detailed analyses of each kind of countermeasure from the point of view of the fundamental physics underlying them. The analyses in that report are for a ground-based strategic defense system. Since THAAD operates in a similar fashion, these measures also can be used to counter a THAAD-like defense system operating in midcourse.³⁵ In this section, we will discuss the effectiveness of three countermeasures in terms of their effect on the kill probabilities: infrared stealth, radar jamming, and decoys. These measures work not just during the endgame, for instance, decoys may cause trouble for EWRs or GBR tracking before the interceptor is launched or during midcourse flight. However, we analyze only their effect on the endgame flight, since our simulation model is an endgame model.

Infrared stealth. Any measures that reduce the target IR radiation level in certain bands can be used as infrared stealth methods. Since the radiation intensity decreases with distance, for a certain signal to noise ratio requirement for the detector, there is a minimum acquisition range at which the target becomes visible to the detector. Therefore, infrared stealth can decrease the acquisition range and thus decrease the KV's available divert time. Since a THAAD-like kill vehicle is guided only by an infrared sensor during its endgame flight, it is possible that infrared stealth could defeat it.

Infrared stealth can be implemented by several means, such as using low-emissivity coatings or a cooled shroud.³⁶ The *Countermeasures* report has already concluded that a warhead cooled to 77 K (liquid nitrogen as coolant) would defeat the NMD KV, but did not look at the effects of higher temperature. To demonstrate how the kill probability varies with the target temperature, the acquisition range of our THAAD-like KV for targets with temperatures from 100 K to 300 K has been calculated in Appendix C. Then series of Monte Carlo simulations of the kill probability were performed at different temperatures, or nominal acquisition ranges. Each simulation contains 1000 runs. All the parameters are the same as the last simulation except that the target speed is set at 5 km/s and 7 km/s, and nominal acquisition ranges are from almost 0 km to 120 km. The results are shown in Figure 10.

The results show that our THAAD-like model's kill probability in both the 7 km/s and 5 km/s cases stays at 100% when the temperature is over 260 K, which corresponds to about a 50 km acquisition range, and then starts to decrease. Above this 50 km acquisition range, even though the KV runs out of fuel in a few cases, the kill probability remains 100%. This indicates that a minimum of a 50 km acquisition range is necessary for a high kill probability. The kill probability decreases quickly from 100% to near zero as the target

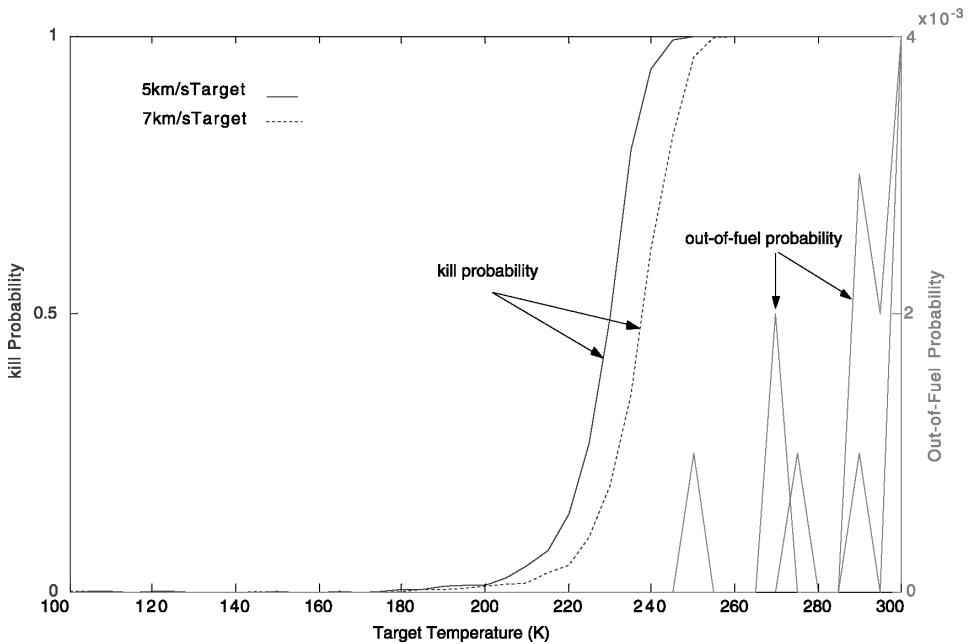


Figure 10: Kill probability and out-of-fuel probability vs. target temperature. The figure shows the kill probability drops when the target temperature drops (which leads to the KV acquisition range and therefore TOF drop) because the KV does not have enough time to maneuver.

temperature goes down from 260 K to 200 K, where the acquisition range drops from 50 km to about 10 km. This result indicates that a target temperature under 200 K is low enough to defeat our KV model. Figure 10 also shows that when temperatures drop down under 240 K, the KV never runs out of fuel, indicating that the cause of the decrease in kill probability is due to a lack of available time for homing, not a lack of fuel.

Comparing the 7 km/s and 5 km/s targets, Figure 10 shows that the kill probability against the 7 km target drops slightly before it does against the 5 km target as the temperature goes down. But the difference is at most 10 degrees. This shows that, in this specific scenario, where maneuver time is the critical factor, a lower closing velocity does help to increase the kill probability, but not very much, and the KV runs out of time due to the short acquisition range against both targets.

So, cooling the target to decrease the IR sensor's acquisition range is effective in defeating our KV model. This model is able to deal only with targets for which it has an acquisition range of at least 50 km. Depending on their

design, other IR homing hit-to-kill KVs are likely to have same problem when encountering an IR stealthy target, although the temperature needed to defeat the KV might be quite different.

The simulation results show that the temperature of the target below which a defense fails is about 200–260 K. This low temperature could even be achieved without using a cooled shroud. It could be achieved by enclosing the warhead in a balloon coated with certain paint. For example, according to the *Countermeasures* report, a balloon with white paint has an equilibrium temperature of 227–241 K in sunlight. This indicates that such passive cooling methods could defeat our KV model as well. Furthermore, the precise target temperature at which the KV could be defeated depends on the details of the KV. This might be a reason why the KV's detection range should be classified.

Decreasing the IR signal would also be done by decreasing the size of the target. Russian nuclear warheads are likely to be smaller than possible nuclear warheads of “countries of concern.” So, some argue that TMD should not be a concern to Russia. But in Appendix C, the target surface area we use to calculate detection range is 1.8 square meters (equivalent to a 1.8 m cone with 0.54 m base diameter), which is comparable to the surface area of an advanced strategic warhead. The 120 km acquisition range of our KV against such a target at room temperature gives a 100% kill probability. This shows that our THAAD-like model can deal with a relatively small strategic warhead that is not using any countermeasures.

Radar Jamming. Since the KV's capability for removing ZEM error is limited by its fuel and TOF, the intercept might fail if the ZEM error is beyond KV's maneuvering capability. Therefore, an essential requirement for the THAAD GBR's performance is to ensure a ZEM error smaller than the required value.

However, the GBR performance might be degraded by radar stealth technology (using radar-absorbing material, for instance)—this would reduce the S/N at a given range—or by electronic countermeasures, such as jamming. A moderate radar degradation could increase target lateral position errors and velocity errors but not necessarily produce a large ZEM. We have already discussed such a case in Example 4. A severe degradation could lead to a large ZEM error, causing the endgame flight to begin with a ZEM error larger than expected, and possibly even larger than that KV can handle. Here we do not attempt to assess how the ZEM error is affected by radar jamming, we only assume ZEM errors as results of radar jamming in order to see how the kill probability varies with ZEM error. Large ZEMs may require the use of more than one jammer.

All the parameters are the same as those in the previous example, with the exception that acquisition range is set to 100 km, and ZEM error is set

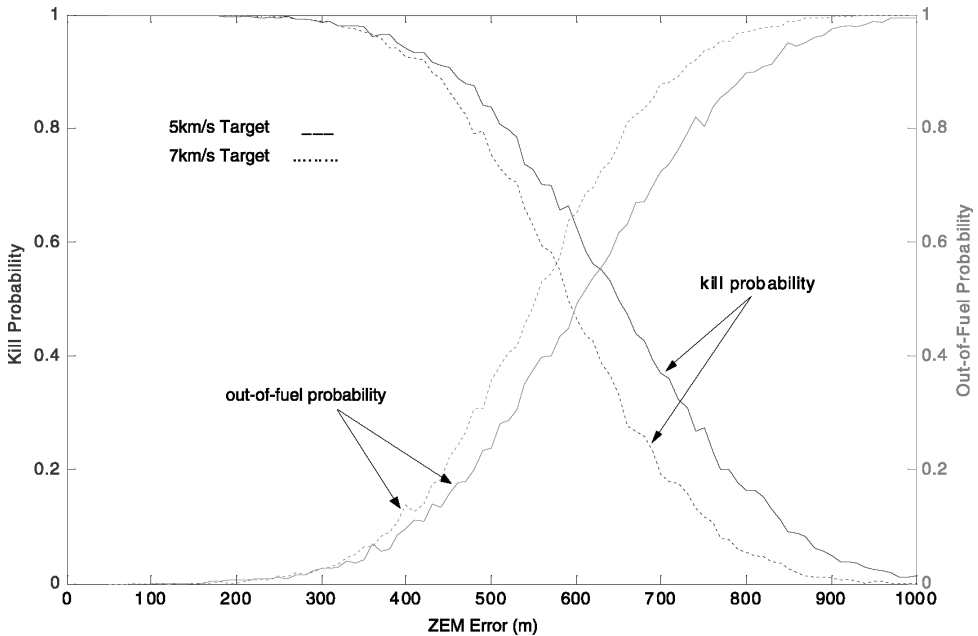


Figure 11: Kill probability and out-of-fuel probability vs. ZEM error. Radar jamming increases the ZEM error and thus decreases the kill probability. The figure shows the kill probability drops to almost zero as the assumed ZEM error is increased from 0 to 1000 m due to jamming. The miss is mainly due to the lateral position and velocity errors are too large to be removed by the given fuel.

between 50 m and 1000 m, with a Gaussian distribution. The results are shown in Figure 11.

We can find from Figure 11 that in both the 5 km/s and 7 km/s cases, the kill probability decreases as the ZEM increases, and the out-of-fuel probability increases with the ZEM. The kill probability remains near 100% when the ZEM is smaller than 300 m, and it drops to almost zero as the ZEM increases to over 1000 m. This shows our KV model can handle about 300 m ZEM at most. Moreover, the miss probability is just a little lower than the out-of-fuel probability. This means that most failures are due to a lack of fuel. This fact also indicates that a lack of fuel does not necessary mean a failure, which agrees with our previous simulation result.

Results are similar against 5 km/s and 7 km/s targets. The only difference is that for the 5 km/s target the kill probability drops about 50–100 m later than 7 km/s target, which means the KV is more robust in dealing with ZEM errors against lower velocity targets.

The results suggest that the ZEM error is a key factor that influences the kill probability. Although our KV model can handle some degradation, characterized by position and velocity errors, radar jamming that induces a large ZEM error would be an effective way to decrease the effectiveness of KV's maneuver capability, and thus cause a catastrophic failure.

Decoys. Decoys or false targets can have almost the same physical characteristics, such as radar cross section (RCS), temperature, and speed, of the real target, or antisimulation techniques could be used to disguise the warhead (see *Countermeasures* report). So the defense system may be deceived by decoys and may guide the KV to the wrong target. However, if the infrared seeker or THAAD radar could discriminate the real target from the decoys, the KV could be commanded to switch to the real target.

To pick out the warhead from deliberately designed decoys is one of the most challenging technical problems to the development of a missile defense system. In this article, we do not further discuss how to distinguish decoys; instead, we will focus on how the kill probability is affected by the spacing of decoys and the time when they are distinguished.

The NMD KV is required to discriminate the real warhead from the decoys, independent of other sensors.³⁷ We assume our KV must similarly be able to discriminate it using its onboard sensor. For the onboard IR sensor, there are two ways to deal with this problem. One is to pick out the target based on its appearance as imaged by the sensor if there is sufficient space between the target and decoys (otherwise, the target and decoys may be in an overlapped FPA area); the other is to distinguish it by analyzing a nonimaged IR signal. Neither may be viable if the decoy is well designed. However, let's first assume the real target can be identified by infrared imaging. The discrimination distance R_D can be approximated by:

$$R_D = \frac{L}{\sin(n_{\min}/n_{\text{FPA}} \cdot \theta)}, \quad (3)$$

where L is geometric size of the target, n_{\min} is minimum number of pixels in one direction needed to discriminate the target, n_{FPA} is the number of elements in one direction of infrared FPA, and θ is the FOV. From experience, the minimum number of imaging pixels needed to discriminate is about 8×8 pixels.³⁸ For a THAAD IR detector of 1 degree FOV and 256×256 pixels FPA, the largest discrimination distance of a 1 m target in diameter is only about 1.8 km, which leaves the KV less than 1 second to go. However, in our discussion of Figure 10, we know that a 50 km detection range is required to assure a successful hit. Therefore, even if the KV's infrared

detector is able to tell the difference between a decoy and a real target by their differences in appearance, it is impossible for a KV with characteristics such as those assessed here to maneuver to a successful hit in such a short time.

Another way for the KV to pick out the target is by differences in its non-imaged IR signal. For instance, the current NMD KV observes signal fluctuations of targets. This requires observing the target's fluctuations for some time, probably at least several seconds. So, a large acquisition range is necessary to do this. More importantly, the target and decoy must be far enough apart to appear to occupy different pixels in the sensor's FOV. This means for a 100 km acquisition distance, the lateral separation must be less than 1.75 km for both to be in the FOV simultaneously and larger than 6.8 m to be sure they can be resolved as separate targets. So, the decoy problem can be characterized by the lateral distance between the target and decoys and by the distance between the target and decoys in the range direction when discrimination occurs.

The first simulation for a decoy scenario is to examine the time when discrimination occurs. But instead of time, we use the distance between the target cluster and the KV to characterize this problem. We consider a decoy 200 meters away from the real target in the lateral direction. Both have the same range and are simultaneously in the infrared detector's FOV. All other parameters are the same as those in the previous simulation example except the ZEM error is set back to 150 m. Discrimination distances are from 23 km (the minimum distance at which both target and decoy are in KV's FOV) to 100 km. Before discrimination occurs, the KV aims at the decoy; when the discrimination occurs, the KV needs to redefine its LOS 0.1–1.0 degree (depending on the time the discrimination occurs) away from its current LOS in order to aim at the real target.

The results in Figure 12 show that the kill probability remains almost zero when the discrimination distance is less than 30 km. Then the kill probability increases quickly with discrimination distance until this distance is about 60 km. From that point on, it remains 100%. The failures are caused either by running out of fuel or by lack of time. Figure 12 also shows that the kill probability against the 7 km/s target drops to zero at about a 10 km larger discrimination distance than against the 5 km/s target, indicating that the KV is somewhat more capable of dealing with a lower closing velocity target when decoys are involved. But both targets have the same catastrophic failure at short discrimination distances.

Another simulation example with decoys is done by varying the lateral distances between the target and the decoys from 100 m to 600 m. All the

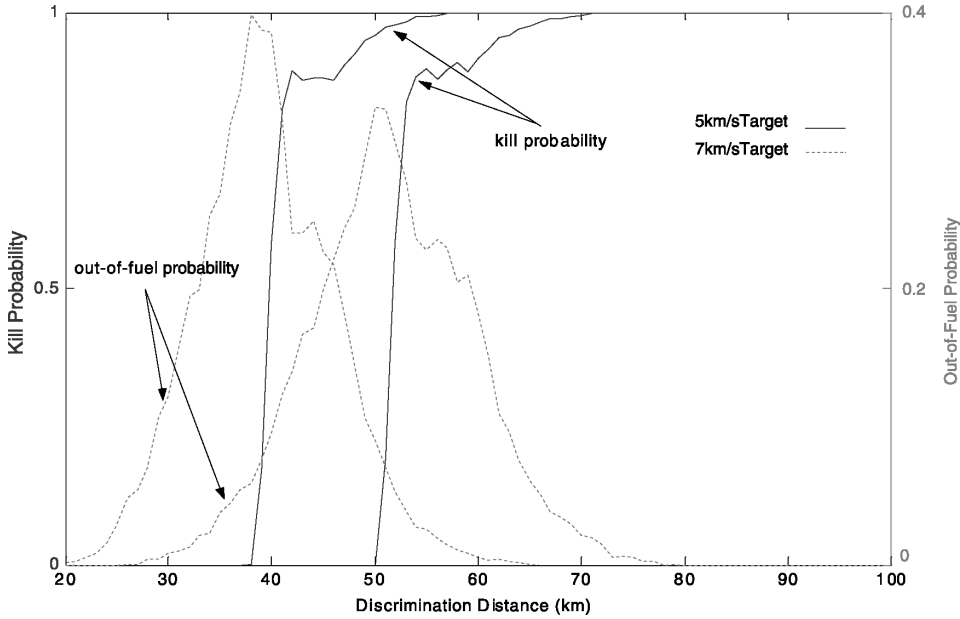


Figure 12: Kill probability and out-of-fuel probability vs. decoy discrimination distance (150 m lateral distance). The results show, for a decoy about 200 m away from the target laterally, the KV discrimination distance has to be at least 70–60 km, depending on the target velocity. Otherwise, the miss could be caused by either running out of fuel or running out of time.

other parameters are the same as those of the previous simulation, except that the discrimination distance is set to 80 km. From the results in Figure 13, we can see that the kill probability remains 100% when the lateral distance is less than 240 m or 280 m, respectively; then it decreases with lateral distance to zero when the lateral distance is over 500 m or 600 m, respectively. The decrease in kill probability is due to an increase in the probability of out-of-fuel. The two targets follow the same pattern with the decrease to zero kill probability occurring about 100 m later for the 5 km/s target.

In general, the simulation shows the KV has the ability to retarget the real target and guide to a successful intercept after discriminating the target. But a large discrimination distance (over 35 km to 45 km) and a small lateral distance between the target and decoy (less than 240 m to 280 m) are necessary for our KV to maneuver to a hit. And again, a lower closing velocity helps to neutralize decoy problems in a minor way.

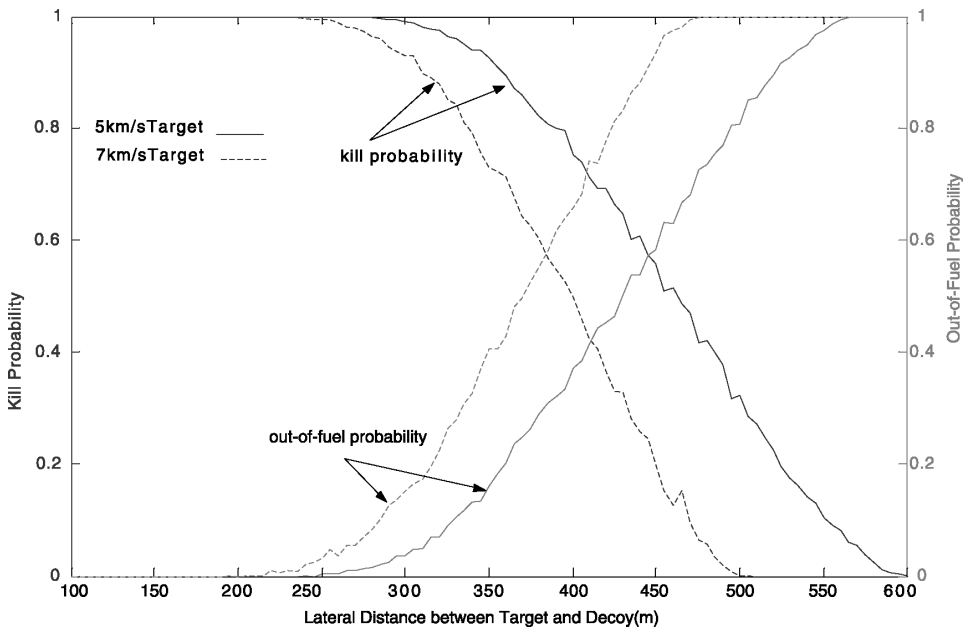


Figure 13: Kill probability and out-of-fuel probability vs. lateral distance between decoy and target (80 km discrimination distance). The results show, for a decoy discriminated at 80 km distance in range direction, the kill probability drops as the lateral distance between the target and the decoy increases due to the KV running out of fuel.

DISCUSSIONS AND CONCLUSIONS

A strategic target could stress a midcourse hit-to-kill defense more than a theater target does due to its higher speed. For example, a higher speed target can compress the defense's battle space by shortening the time interval between first and last intercept opportunities. This could make an effective defense against strategic targets more difficult. However, in the endgame homing process, there are many parameters that affect the kill probability. The most important ones are the PIP error, the interceptor's divert capability, the TOF in endgame, the seeker's angle measurement accuracy and frequency, and the dynamic responses of divert thrusters to divert commands. Since the closing velocity is a parameter that only affects the TOF, it is likely that some parameters of a theater defense can be traded off to enable the defense to be capable of dealing with strategic threats as well.

The miss distance and kill probability analyses in this article show that the performance assumptions that we have made for the seeker, divert, and GBR subsystems of a THAAD-like system meet the requirements for engaging both

theater and strategic missile targets. If a missile defense system satisfies all the performance assumptions made herein, no malfunctions occur, and no serious countermeasure is present, it has a kill probability of almost 100% against both a target missile moving at 5 km/s and a target moving at 7 km/s. The difference in the KV's kill probability against a theater target and a strategic target lies only in the difference of divert capability due to the difference in the TOF. However, the simulation results show that the miss distance is not very sensitive to TOF errors (up to 0.1 second), and that the endgame performance is quite robust against inaccuracies in the initial condition information provided to the KV at acquisition. In our simulations, all the misses are caused by lack of fuel or diverting capability if no countermeasures are present. So, the KV can almost always hit the strategic target if it is capable of hitting a theater target.

The above discussion clearly demonstrates that a THAAD-like defense system is able to intercept a strategic target. It also indicates that the effort made in the now abandoned TMD Demarcation Agreement to prevent a TMD system from acquiring a strategic capability by limiting only the target velocity could not succeed. So a THAAD-like high altitude TMD system could be used as a strategic defense system, and thus U.S. strategic defense capability would be determined not only by its planned strategic defense system, but also by its high altitude TMD systems, like THAAD. In these cases, it makes no sense to discuss U.S. strategic defense capability based only on its number of NMD interceptors.

The performances of external sensors and of the KV itself are key factors in determining the capability of high altitude TMD systems to perform strategic intercepts. In practice, the variation of the PIP error with time is a very important specification that is determined by the performances of external sensors. It is one of the main factors that not only determine the size of the defense's footprint, but also the kill probability in a given engagement. The PIP error determines how much time an interceptor has to fly out because an interceptor usually is launched after the PIP error begins to fall below the interceptor's maximum lateral diverting distance.³⁹ If the PIP error is too large, the kill probability would be lowered due to a higher probability of running out of fuel before the KV is put on a collision course, even though the seeker subsystem can still get an accurate estimate of the position of the target.

The simulations also show that current DSP and EWR information is accurate enough for a THAAD-like high altitude defense system to intercept a strategic target successfully during endgame flight. With future, more accurate, space-based cueing and tracking information, or use of NMD GBRs, such a THAAD-like defense system could have capabilities even more similar to those

of a strategic defense system. So, with all the external sensors incorporated into this kind of TMD system, it is likely that a limited strategic defense capability could be turned into a much larger capability on a short notice, which could change the political implications of U.S. missile defenses dramatically.

Countermeasures are a very complex issue and involve many factors. The theoretical computation in this article shows preliminarily that even partially effective countermeasures could defeat a KV's endgame homing process.

The simulations show that the KV's failures in dealing with countermeasures are due to a lack of either time or fuel. This indicates that the KV's capability of dealing with countermeasure is determined by both its fuel and acquisition range. A KV carrying more fuel with onboard sensor capable of detecting target at a larger distance would be more capable of dealing with countermeasure problems. This is partly why a more capable sea-based KV with greater detection range and more divert is said to be needed if it is to be used for NMD.⁴⁰ This over-design strategy helps to deal with unpredictable errors. It provides the KV greater capability to remove errors in endgame flight. However, this over-design is always limited. It could be overwhelmed by a larger error created by a countermeasure. Depending on how robustly the KV is designed, TMD used as strategic defense may be much more vulnerable than the NMD KV is. So, it is unlikely that a definitive solution to the countermeasure problems will be to over-design the TMD KV.

Moreover, this preliminary conclusion on the countermeasure problem drawing from an endgame game homing process simulation could also be true for a strategic defense system. A strategic defense KV would have more maneuver capability. But based on the same fundamental principle, the countermeasures we mentioned in our simulation could still raise questions about its endgame homing capabilities by creating larger endgame maneuver requirements. Our computations already demonstrate that a high altitude theater defense has almost the same kill probability against theater and strategic targets. Therefore, the principle behind a countermeasure effective against a theater defense system can be expected to be able to work against strategic defense system as well, although the size of the effect produced by the countermeasure may need to be larger. So, the countermeasures of the type we discussed in our simulation could also be effective against strategic defense system.

NOTES AND REFERENCES

1. The kill probability is determined by both the hit probability and the destruction probability in an attempt engagement. Since the kill mechanism under hit to kill technology is beyond the scope of this article, we assume the target is definitively killed

once hit by the kill vehicle. Therefore, the hit probability is taken as the kill probability herein.

2. Lisbeth Gronlund, George Lewis, Theodore Postol, and David Wright, "Highly Capable Theater Missile Defenses and the ABM Treaty," *Arms Control Today* Vol. 24, No. 3, April 1994, 3–8.

3. C.B. Chang presented an analytical model intended for sensor and interceptor trade-off analysis with some important factors incorporated. The simulation results of the model show that, although the miss distance increases with increasing closing velocity, the degradation of the miss distance with increasing closing velocity under the given parameters is not severe enough to prevent an interceptor capable of hitting a long-range theater target from hitting a strategic target. See C. B. Chang, "A Model for Sensor-Interceptor Trade-Off Analysis," Technical Report 599, Lincoln Laboratory, Massachusetts Institute of Technology, 18 January 1982.

4. The purpose of aim point selection is to aim the KV at a specific lethal point on a target. It begins when the target IR image exceeds at least one pixel in size.

5. Robert W. Bass et al., "Establishing Requirements for Homing Applications," *Proceedings of the SPIE, Vol. 1339, Materials, Devices, Techniques, and Applications for Z-Plane Focal Plane Array Technology II*, San Diego, CA, USA, 12–13 July 1990, 53–76.

6. George Lewis and He Yingbo, "U.S. Missile Defense Activities and the Future of the ABM Treaty," *Physics and Society* Vol. 27, No. 1 (January 1998), 8–10, also see Lisbeth Gronlund et al., *Arms Control Today*, Vol. 24, No. 3, April 1994, 3–8.

7. For instance, in 1994, then Director of the BMDO, General Malcolm O'Neill, showed the U.S. Senators a defended footprint for THAAD against an ICBM. He later stated that "...Analysis indicated that in one-on-one engagements against RVs deployed on some strategic missiles, THAAD, if cued from space, would have a capability to counter a non-trivial portion of Russia's strategic force."

8. Based on the idea that a strategic target traveling at a higher speed would present a serious problem for a defense system that has only been tested against targets flying at a lower speed, the now-abandoned TMD Demarcation Agreements set a target velocity of 5 km/s (equivalent to a range of 3500 km) as the maximum speed allowed for TBM targets under the ABM Treaty. The government negotiators may have assumed that a 25–30 percent increase in the closing velocity would cause a sharp drop in the kill probability, rendering a TMD system ineffective against strategic missiles even if its kill probability against theater targets is high in flight tests.

9. The material used in this section that is not otherwise cited comes from the following sources: Ballistic Missile Defense: 12 Years of Achievement, Prepared statement of Lt. Gen. Malcolm R. O'Neill, USA, BMDO, to the House National Security Committee, 4 April 1995; THAAD home page at (<http://www.lmsw.external.lmco.com/thaad/>).

10. The THAAD is now being reengineered, but this does not significantly affect our analysis because we are only looking at a THAAD-like system.

11. Although during the Clinton administration the United States said that it would not deploy THAAD on U.S. territory for strategic defenses, it is highly mobile and could be rapidly deployed anywhere in the United States.

12. FOV is different from the field of regard (FOR), which is defined as the maximum angle that the seeker can scan by tilting its gimballed platform.

13. This is a user operational evaluation system (UOES) configuration. It was available at BMDO (Ballistic Missile Defense Organization) home page: (<http://www.acq.osd.mil/bmdo/bmdolink/pdf/38112.pdf>). The UOES is not the actual version that will be deployed. As noted before, this is not a serious concern, since we are interested in assessing the relative performance of a THAAD-like interceptor, not the actual THAAD.
14. Later, we will see the KV's σ lateral position error is about 25 m when the endgame starts. So a 3σ distribution of the handover error leads a 150 m diameter error circle.
15. Michael A. Dornheim, "THAAD Second Source Unlikely, Army Says," *Aviation Week & Space Technology*, 24 March 1997, 33.
16. Charles D. Brown, *Spacecraft Propulsion* (Washington: American Institute of Aeronautics and Astronautics, 1996).
17. D. Ruttle et al., "Development of miniature 35-LBF fast response bipropellant divert thruster," AIAA 93-2585, AIAA/SAE/ASME/ASEE 29th Joint Propulsion Conference and Exhibit, 28–30 June 1993, Monterey, CA.
18. Theodore Postol, "Estimated Properties of THAAD Interceptor," working paper.
19. This is the average divert velocity in two directions. In reality, the KV could spend more fuel for divert in a certain direction if necessary.
20. Given this thrust, the acceleration will be slightly higher at the end of divert because the KV is lighter, but we neglect this.
21. Here, the divert thrusters are assumed not to be throttleable.
22. "Nominal" here means as known to the defense system.
23. The coordinate system chosen for a real defense system must be more general and more complicated, but the choice of a coordinate will not affect the basic physical law we are going to explore.
24. The closing velocity is defined as the negative rate of change of the distance from the KV to the target.
25. The formula used for calculation is $\delta_R = c/4\beta\sqrt{S/N}$, and assumes the bandwidth $\beta = 1$ GHz to be 10 percent of the radar frequency. For more detailed discussion, see J. C. Toomay, *Radar Principles for the Non-Specialist* (New Jersey, Scitech Publishing Inc. and Washington, SPIE OPTICAL Engineering Press, 1989, second edition), 87.
26. "Multiple Target Engagement Capabilities of a THAAD GBR Radar Operating in an ABM Mode," Theodore Postol, working paper. Quoted with author's permission.
27. Actually, the divert acceleration is normal to the KV's longitudinal axis, so the most efficient way of using the divert is to align this axis with the instantaneous LOS. Because of the position of the seeker's window, there may be an angle of 5° to 15° between the KV's axis and LOS. This then does contribute to a change of the range rate and the thrust along the Y axis. The contribution of that small angle to the thrust along the Y axis can be compensated for, because the angle is known to the IAP. The change of range rate will be far less important than the error in estimating the closing velocity.
28. The detection range calculation in Appendix C shows that the FPA's performance supports a data update rate of 50 Hz for a 120 km acquisition range.

29. In the article "Hughes gets ready to launch its LEAP version," *SDI Monitor*, 28 February 1992, an acquisition range of 100 to 200 km against an RV for a mercury-cadmium-telluride detector is claimed. As mentioned in Appendix B, Raytheon claims that the current Aegis LEAP has an acquisition range of over 300 km. The KV of the current land-based midcourse interceptor (former NMD interceptor) has a larger acquisition range.
30. More detailed description of the Kalman filter can be found in: Paul Zarchan, *Tactical and Strategic Missile Guidance* (Washington: American Institute of Aeronautics and Astronautics, Progress in Astronautics and Aeronautics, Vol. 176, Third Edition, 1996); Arthur Gelb, *Applied Optimal Estimation* (The MIT Press, May 15, 1974).
31. The thrust normal to the instantaneous LOS may be less than a thruster's actual value because the KV's longitudinal axis may deviate from the LOS. This can be compensated for because the KV's attitude is known.
32. D. Ruttle et al., "Development of miniature 35-LBF fast response bipropellant divert thruster," AIAA 93-2585, AIAA/SAE/ASME/ASEE 29th Joint Propulsion Conference and Exhibit, 28–30 June 1993, Monterey, CA.
33. From now on, we refer to the amount of fuel used by doubling the fuel consumed in one direction when we discuss the fuel consumed.
34. Andrew M. Sessler et al., *Countermeasures: A Technical Evaluation of the Operational Effectiveness of the Planned U.S. National Missile Defense System* (Union of Concerned Scientists/MIT Security Studies Program, Cambridge, MA, March 2000).
35. THAAD can also operate in the upper layers of the atmosphere where some countermeasures, such as lightweight decoys, will no longer be effective.
36. George N. Lewis and Theodore A. Postol, "Future Challenges to Ballistic Missile Defense," *IEEE SPECTRUM* (September, 1997); or Andrew M. Sessler et al., *Countermeasures: A Technical Evaluation of the Operational Effectiveness of the Planned U.S. National Missile Defense System* (Union of Concerned Scientists/MIT Security Studies Program, March 2000), 81–90.
37. See the unclassified "Independent Review of TRW Discrimination Techniques Final Report," Phase One Engineering Team (POET) Study 1998–5.
38. Zhong Renhua, *Infrared Missile Guidance System* (Beijing: Aeronautic and Astronautic Press, September 1995, in Chinese).
39. The defense can also launch interceptor when PIP is still larger than KV's maneuver capability. This extends the defense footprint at the cost of kill probability if no other measures are adopted to reduce PIP (for example, reducing the PIP by the maneuvers of interceptor's booster).
40. "Upper Tier Supporters Eye National Missile Defense Role," *Inside Missile Defense*, September 27, 1995.
41. Similar analysis for a 3,500 km range theater target shows the PIP updates history are within our assumption value based on this 10,000 km strategic target. In the theater target case, the interceptor should be launched 10 seconds later than against strategic target; Moreover, the EWRs and the GBR have 120 s and 30 s more tracking time, respectively, because of the slower closing velocity.
42. Moshe Weiss and Theodore Postol, "Vulnerabilities of U.S. National Missile Defense Radars to Countermeasures," MIT Security Studies Program Working Paper.

43. The following equation is used for scaling of tracking distance: $S/N = P_{ave} t_0 G^2 \lambda^2 \sigma / (4\pi)^3 R^4 K T_s L_s$. If the target is approaching on a near radial trajectory (which will depend on the size of the area being defended), the maximum search range is obtained when the search time is chosen to be proportional to the required minimum detection range. In this situation, the detection range is proportional to the cubic root of the S/N .

44. Having enough tracking measurements is one of the most important factors for achieving a high tracking accuracy. However, the EWR may have to track multiple targets simultaneously. Therefore, the number of measurement for a specific target is limited in a given tracking period. 90 seconds is not long enough for 20 measurements with 10-second revisit time used in Weiss's calculation; however, the EWR can still have 20 sample measurements by adjusting its revisit time.

45. Lisbeth Gronlund et al., "Highly Capable Theater Missile Defenses and the ABM Treaty," *Arms Control Today*, Vol. 24, No. 3, April 1994, 3–8.

46. Here, the author conservatively assumes that the detection range for the search radar is inversely proportional to the fourth root of the solid angle of the area needed to be searched, instead of the cubic root. For the latter case, a detection range of 1027 km is obtained.

47. The formula used to obtain the accuracy of the radar measurements is $\delta_\theta \cong \lambda / 2D \sqrt{S/N}$, see J. C. Toomay, *Radar Principles for the Non-Specialist* (New Jersey, Scitech Publishing Inc. and Washington, SPIE OPTICAL Engineering Press, 1989, second edition), 58. Here a square radar antenna with 9.2 m area is assumed.

48. J. C. Toomay, loc. cit.

49. Raytheon Company, "TMD-GBR Overview," News briefing slides, 19 May 1995.

50. The angular prediction error could be estimated by $\varepsilon_\sigma \approx \sqrt{2} \cdot \Delta\theta \cdot (1 + \frac{2T}{t})$, where T is the time ahead predicted, and t is duration of the measurement. See J. C. Toomay, op. cit., 59. In our case, T and t are 30 s (or 60 s) and 50 s, respectively.

51. Michael A. Dornheim, "Loss of Position and Velocity Data Makes SDI LEAP Interceptor Miss Target," *Aviation Week and Space Technology* (29 June 1992), 66.

52. Ben Iannotta, "Target Error Again Gets Blame in 2nd LEAP Test Failure," *Defense News* (12–18 July 1993), 20.

53. "LEAP Suborbital Flight Cleared," *Aviation Week & Space Technology* (31 August 1992), 71. The weight here is 2 kg higher than that in Table B-1.

54. "Strategic Defense Initiative: Some Claims Overstated for Early Flight Tests of Interceptors," United States General Accounting Office, GAO/NSIAD-92-282 (September 1992), 27.

55. James R. Asker, "SDI Shows Solid-fuel Projectile, Seeks Navy Tests in LEAP Program," *Aviation Week & Space Technology* (6 January 1992), 49. "LEAP Suborbital Flight Cleared," *Aviation Week & Space Technology* (31 August, 1992), 71.

56. Kinetic Kill Vehicle Flies in Hover Test, *Aviation Week & Space Technology*, Newsbreaks (5 March, 1994).

57. See (<http://www.raytheon.com/es/esproducts/dssleap/dssleap.htm>), 14 March 2002. The divert distance depends on both divert velocity and endgame flight time. For a given KV, a larger divert distance could be achieved by having longer endgame flight time. So, this 3 km divert distance does not necessarily mean the KV has very high maneuver capability. It is really divert velocity that counts.

58. Bob Aldridge, "From Star Wars to Scud Buster: A Background Paper on Ballistic Missile Defense," Pacific Life Research Center, 20 April 2000. Online at (<http://www.nuclearfiles.org/replrc/Ballistic%20Missile%20Defense3.pdf>).
59. "Navy considering Liquid Propellant for Missile Defense Booster," *Inside Missile Defense*, 11 July 2001.
60. Hughes and Rockwell are the two companies that started the EKV research and development in early 1990s. Raytheon bought Hughes in 1997. Raytheon's kill vehicle sometimes is called the Raytheon/Hughes kill vehicle. Boeing bought Rockwell in 1996. The Boeing kill vehicle is also called the Boeing/TRW kill vehicle since TRW develops target discrimination software for the Boeing kill vehicle.
61. DOD news briefing: "MG Nance Provides Update on Missile Test," available at (<http://www.defenselink.mil/news/Aug2001/t08092001.t809bmdo.html>).
62. The divert velocity estimated here is the maximum value, because part of the fuel has to be used in attitude control.
63. William B. Scott, "Data Boost Confidence In Kill Vehicle Performance," *Aviation Week & Space Technology* (8 June 1998), 57.
64. THAAD is also intended to make intercepts in the upper layers of the atmosphere. Estimating the detection range in this case is more complex because both the target and the seeker window will be heated by atmospheric friction.
65. Early test versions of the THAAD interceptor used a PtSi array, which is easier to fabricate. However, the sensitivity of PtSi is much lower, with a quantum efficiency of only a few percent (compared to 60 to 90 percent for InSb).
66. The information on InSb in this paragraph is taken from John Lester Miller, *Principles of Infrared Technology* (New York: Chapman and Hall, 1994), 156–158. The cutoff wavelength of $5.6 \mu\text{m}$ is for an array at 77 K, it will decrease as the array is cooled further.
67. Miller, *op. cit.*, 177–192.
68. Devon G. Crowe, Paul R. Norton, Thomas Limperis, and Joseph Mudar, "Detectors," in William D. Rogatto, ed., *The Infrared and Electro-Optical Systems Handbook*, Vol. 3: *Electro-Optical Components* (Ann Arbor, Michigan and Bellingham, Washington: Infrared Information Analysis Center and SPIE Optical Engineering Press, 1993), 224.
69. William L. Wolfe, "Optical Materials," in William D. Rogatto, ed., *The Infrared and Electro-Optical Systems Handbook*, Vol. 3: *Electro-Optical Components* (Ann Arbor, Michigan and Bellingham, Washington: Infrared Information Analysis Center and SPIE Optical Engineering Press, 1993), 14.
70. William L. Wolfe, "Properties of Optical Material," in Walter G. Driscoll and William Vaughan, eds. *Handbook of Optics* (New York: McGraw-Hill, 1978), 7–47 (Figure 1.16).
71. Miller, *Principles of Infrared Technology*, 188–189.
72. Thomas B. Cochran, William M. Arkin, and Milton M. Hoening, *Nuclear Weapons Databook*, Vol. 1: *U.S. Nuclear Forces and Capabilities* (Cambridge, Massachusetts: Ballinger, 1984), 75.
73. S.A. Hovanessian, *Introduction to Sensor Systems* (Norwood, Massachusetts: Artech House, 1988), 182. A 256×256 array operating at 50 Hz makes about 3.3 million

detection decisions per second, so on average there will be a false alarm about every three seconds.

74. On average, the warhead emits $8.3/4\pi$ W = 0.66 W per steradian. Viewed base-on, with a base area of 0.23 m^2 , the warhead will emit about $1.06/\pi = 0.34$ W per steradian.

APPENDIX A—TRACKING ACCURACY AND PIP ACCURACY UPDATE

The variation of the PIP accuracy over time is a very important consideration in designing a defense system, since it can be traded off against the KV's maneuvering capability. The PIP accuracy is mainly determined by the performance of sensors external to the KV. This appendix estimates how the PIP accuracy is improved after the target is acquired by different sensors including DSP satellites, EWRs, and GBRs. The following timeline and geometry analyses are based on the trajectory of a 10,000 km range target with an apogee of 1500 km.⁴¹

DSP Satellites

DSP observations on a missile launch can be used to estimate the threat missile state vector and associated error statistics at burnout, which allow predictions of future positions. Any uncertainty in the estimated threat state vector at burnout results in an error ellipsoid associated with the position of the threat at some later time, and nonzero components associated with the burnout velocity vector uncertainty cause the error ellipsoid to grow with time. DSP is not sufficient for predicting the PIP, due to both its relatively low tracking accuracy and the long time ahead it needs to predict. However, DSP satellites are useful for providing early warning of a missile launch and cueing the EWRs, the THAAD GBR, and possibly the NMD GBR in an attack aimed at U.S. territory, or cueing only the THAAD GBR in a situation in which information from other sensors is not available. In an attack on U.S. territory considered here, the DSP tracking information is assumed to be the only information on the target missile available to the THAAD defense system before the EWR detects the target.

EWRs

The current U.S. early warning radars surrounding U.S. territory can provide the THAAD system with high quality PIP estimates. There are many possible geometries in a real engagement. Here we assume the intercept is to take place about 240 km downrange from the interceptor's launch site (which is different from but close to the missile's impact point) and at an altitude of about 100 km, then according to flyout contours for a THAAD-like interceptor produced by Theodore Postol (see Figure A-1), it takes about 150 seconds for the THAAD

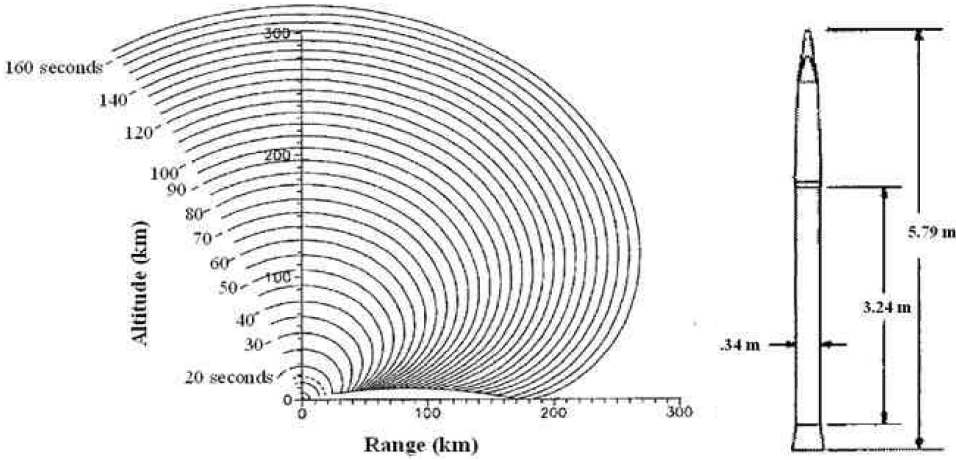


Figure A-1: Flyout contours of the baseline THAAD interceptor: accelerates for 17 seconds, launch gross weight 1263 lbs., missile weight at burnout = 300 lbs., specific impulse = 250 seconds, thrust = 14,164 lbs., acceleration at liftoff = 11.2 g.

interceptor to cover that distance. Thus, to reach that point, the interceptor has to be launched when the target is still 1,300 km away from the interceptor launch site.

Moshe Weiss has studied the tracking, estimation and prediction accuracy of an improved Pave Paws EWR located at 600 km up-range (that is, the warhead flies over the radar) from the impact point of an ICBM warhead with a RCS of 0.05 m^2 on a lofted trajectory.⁴² It is assumed that the radar beam dwell time is 0.064 seconds per look with a 10-second revisit time, and 20-measurement looks are gathered in 200 seconds. Under these conditions, he concludes that the EWR can start tracking when the target is about 2,000 km away from the EWR and the standard deviations (SD) of the impact point estimates and the velocity estimates are 1.29 km and 1.8 m/s, respectively, when tracking is completed. For a typical strategic target with a RCS of 0.005 m^2 then, the EWR should be able to start tracking at a range of at least 1100 km with all other conditions intact.⁴³ If the EWR is located 600 km up-range from the defense, it takes the target about 280 s to hit the ground after being detected by EWR. Thus, when the EWR starts tracking, it is 90 s before the launch of interceptor. If the EWR makes 20 tracking measurements during this time, then the 1.29 km impact point prediction error should be achieved by that time.⁴⁴ Since the error grows with time, the PIP error should always be smaller than the impact point prediction error at a given estimation moment. Therefore, using

the information provided by the EWRs, the THAAD BM/C³I should be able to obtain the PIP with accuracy better than that of the impact point estimates. Based on this judgment, we estimate that the 1σ PIP error should be less than 1.29 km when interceptor is launched.

GBR

As very accurate target trajectory information from the EWR is available to the THAAD GBR, it needs only to search a very small area in the sky. The solid angle of that area can be as small as 0.6×0.6 square degrees, which is roughly the angular beam width of THAAD-like radar. Lisbeth Gronlund et al. estimate that a THAAD-like radar can detect an approaching target with a small RCS (0.005 m^2) at a range of 270 km in a solid angle of 27 square degrees,⁴⁵ so the 0.36 square degrees solid angle would allow a detection range of at least 800 km, which is about the range at which the EWR tracking ends.⁴⁶ If THAAD GBR is assumed to be located at the interceptor launch site, this 800 km detection range means the THAAD GBR should be able to detect the strategic target 70 seconds after the launch of the interceptor. For a signal to noise ratio of 30, which is what Gronlund et al. assume is needed to detect and track the target, a single measurement accuracy of the target's cross-range position would have an accuracy of about 0.001 radians, corresponding to 0.8 km at 800 km range.⁴⁷

The GBR starts tracking efforts after detecting the target. Toomay states that the tracking accuracy of a C band (5 GHz) radar with a 5 meters dish is 0.0001 radians.⁴⁸ Since the beam width of such radar is similar to that of a THAAD-like radar, which is 0.01 radians, this indicates that a THAAD-like radar could have a tracking accuracy of about 0.0001 radians. Furthermore, it is stated in a briefing by Raytheon, the manufacturer of the GBR radar, that the single measurement accuracy for THAAD-like radar is typically one-tenth of the antenna beam width, and the tracking accuracy is one-hundredth of the antenna beam width, or about 0.0001 radians.⁴⁹ Both indicate that a tracking accuracy of 0.0001 radians is a reasonable estimate for a THAAD-like radar. If we assume 50 seconds are needed for the THAAD GBR to complete this tracking process, the tracking accuracy of 0.0001 radians can be achieved 120 s after the interceptor is launched, when the target is roughly 470 km away from the defense launch site. The angular predicting error at PIP is about 0.0003 radians.⁵⁰ So the PIP error should be about 80 m at 270 km distance from radar.

As the target approaches the defense system, the PIP error continues to decrease, due to both improved tracking accuracy and the decreasing distance

Table A-1: The PIP accuracy improvement process.

Time	Sensor	Events	PIP error
≪ -90 s:	DSP	Target launch detected	No PIP available
-90 s:	EWR	Starts tracking	Less than 1.29 km
0 s:		Finishes 20 measurements	
70 s:	GBR	Starts tracking	
120 s:		Achieves 0.0001 rad tracking accuracy	80 m

The target is assumed of 10,000 km range with 1,500 km apogee. The EWR is 600 km uprange from interceptor launch site and the GBR is at the interceptor launch site.

between the GBR and the target. However, the tracking accuracy will improve only slowly after tracking for a certain time, and the target gets only 30 km closer to the GBR at the PIP. So, we neglect this small PIP improvement. Table A-1 summarizes timeline of PIP update.

APPENDIX B—THE LEAP KV AND THE NMD KV

This appendix briefly reviews the other two publicly known major kill vehicles that are under development or have been developed by United State since the Strategic Defense Initiative (SDI) program.

LEAP Kill Vehicle

The Lightweight Exo-Atmospheric Projectile (LEAP) program, initiated in late 1980s by the Strategic Defense Initiative Office (SDIO), was to develop, integrate and test a miniaturized kinetic kill vehicle in order to benefit both space-based boost phase intercept and ground-based intercept. Boeing, Hughes, and Rockwell were the prime independent contractors of the LEAP program.

The LEAP KV flight test record was good in early 1990s until the first intercept was attempted. The first LEAP kill vehicle hover test was made successfully in June 1991. And the first LEAP kill vehicle flight test was successful in February 1992 (no intercept was attempted). However, the first intercept test failed on 19 June 1992 because the target did not transmit its position and speed to the KV to initiate the Kalman filter in its guidance system.⁵¹ The KV also missed the target during the next intercept flight test on 22 June 1993. According to BMDO officials, the target was released about 1 km beyond its intended location.⁵²

The technical characteristics of the LEAP kill vehicles have changed with time and vary between sources. In an SDIO slide, the technical data for

Table B-1: SDIO data on LEAP kill vehicles tested in early 1990s.

	Hughes/Army	Boeing/Air Force	Rockwell/Air Force
Mass (kg)	6	7.3	17
Divert capability (m/s)	420	430	550
FPA	128 × 128 (HgCdTe)	64 × 64 (HgCdTe)	256 × 256 (HgCdTe)
Seeker wave band (micron)	3–5 or 7–9	3–7	4–5 and 8–26
Seeker FOV (deg)	1.1	1.0	3.0
IMU drift (3σ , deg/hour)	<3	<4	<5
Estimate fuel mass (kg)	0.9	1.1	3.1

several versions of LEAP in the early 1990s was given as shown in Table B-1. All the kill vehicles were designed to use liquid fuel for divert. Another source says Rockwell's LEAP kill vehicle weighed about 19 kg, and used a 256 × 256 mercury-cadmium-telluride FPA, with a tracking accuracy of less than 200 μ rad.⁵³ A General Accounting Office (GAO) report said that the Hughes/Army version of LEAP was 152 mm in diameter, 356 mm long, and weighed about 6 kg with fuel; and the Boeing/Air Force and Rockwell/Air Force versions weighed about 10 kg and 18 kg, respectively.⁵⁴ The Rockwell LEAP KV was claimed to have maneuvered at 2–4 g in hover tests, and the Boeing LEAP KV was said to be able to accelerate at 3.5 g.⁵⁵

In 1994, SDIO tested a Hughes solid fuel LEAP projectile.⁵⁶ This version of LEAP weighed 9 kg, of which 4 kg was the solid propulsion system built by Thiokol Corp., Elkton Division. The thruster burned for 16 seconds. If the divert velocity is 420 m/s as shown in Table B-1, and if we assume specific impulse (I_{sp}) of the solid fuel is 220 seconds, then the solid fuel weighed about 1.6 kg.

The current sea-based midcourse defense program, the former NTW program, uses a solid propellant kill vehicle based on the LEAP demonstration program. Raytheon and Boeing North America are the contractor team for this NTW AEGIS LEAP, where Raytheon is responsible for the IR seeker, and Boeing is responsible for the guidance and integration. According to Raytheon, the Aegis LEAP has a wide FOV, large aperture, long-wave IR seeker, over 300 km acquisition range, and over 3 km SDACS divert system.⁵⁷ This so-called third generation LEAP weighs about 9 kg.⁵⁸ The Navy missile defense program is

now considering replacing the solid kill vehicle with a liquid propulsion system to achieve higher performance and greater mission flexibility for energy management.⁵⁹

The two Navy LEAP flight tests in the mid 1990s were both failures. On 4 March 1995, the LEAP failed to hit its target because of a programming error in its guidance system, and LEAP failed again on 28 March 1995 due to a battery failure. However, it achieved good flight results in 2002. LEAP reportedly hit the target three times, on 25 January, 13 June, and 21 November, respectively.

Ground Based Midcourse Defense Kill Vehicle (NMD KV)

There were originally two competing NMD kill vehicles, one by Raytheon and another by Hughes.⁶⁰ In December 1998, the Raytheon version was selected as the primary KV by the then BMDO. According to a BMDO viewgraph from August 1998, the Raytheon NMD EKV has a “tactical weight” of 55 kg. This Raytheon EKV was described as having a “high” divert capability, as compared to the “moderate” divert capability of the Hughes NMD EKV weighing 35–45 kg, which became the backup NMD EKV. Another BMDO fact sheet from November 1998 said the NMD EKV would have 9 to 14 kg of fuel, consisting of monomethyl hydrazine and nitrogen tetroxide. If the higher fuel mass corresponds to the Raytheon version and the lower to the Hughes, then the dry mass of the current NMD kill vehicle is about 41 kg. According to a DOD news briefing on the Integrated Flight Test (IFT) 6 on 9 August 2001, the KV is 1.4 m long, 0.61 m in width, and weighs about 54.4 kg.⁶¹ The weight agrees with that released three years ago.

Assuming the I_{sp} is 270 s, and then using rocket equation, we estimate the Raytheon KV has a maneuver capability of up to about 760 m/s.⁶² The backup KV has a maneuver capability of up to about 600–800 m/s.

The IR detector of the Raytheon kill vehicle consists of 256×256 elements that are cooled to 68–70 K within 60 s by krypton. The kill vehicle has been able to acquire nine dispensed targets at a range of approximately 700–800 km in a flyby test.⁶³

As of December 2002, the NMD KV has had eight intercept tests (IFT-3–IFT-10) since October 1999. IFT-4, IFT-5, and IFT-10 failed due to a cooling system failure, booster malfunction, and booster separation failure, respectively. The other five tests were reportedly successful in hitting the target.

APPENDIX C—ESTIMATING THE DETECTION RANGE OF A THAAD-LIKE SEEKER

George N. Lewis*

Introduction

Here we make a rough estimate of the minimum exoatmospheric detection range of a THAAD-like seeker against a small, strategic RV. By detection range, we mean the range at which the detector will have a specified (high) probability of detection and a specified (low) false-alarm probability. The RV is assumed to be at a temperature of 300 K and the intercept attempt takes place above the atmosphere with the target viewed against a cold space background.⁶⁴

Consider an infrared target emitting power Φ_T within the spectral band of the THAAD seeker. Φ_T is given by:

$$\Phi_T = \varepsilon \cdot A \cdot \int_{\lambda_1}^{\lambda_2} \frac{2\pi hc^2}{\lambda^5} \frac{1}{e^{\frac{hc}{kT}} - 1} d\lambda, \quad (\text{C-1})$$

where ε is the emissivity of the target, A is the surface area of the target, λ_1 and λ_2 are the lower and upper detector wavelength limits, respectively, $h = 6.626 \times 10^{-34}$ (J · s) is Planck's constant, $k = 1.3806 \times 10^{-23}$ (J · K⁻¹) is Boltzmann's constant, $c = 2.9979 \times 10^8$ (m · s⁻¹) is the speed of light, λ is wavelength, and T is the temperature of the target.

Assuming that all the target signal power reaching the aperture of the seeker is focused onto a single detector element, then the power on the detector element is then given by:

$$\Phi_D = \Phi_T A / 4\pi R^2 L, \quad (\text{C-2})$$

where A = optics aperture area, R = range to target, and L = system losses.

This power on the detector Φ_D will be sufficient to detect the target if:

$$\Phi_D = (S/N)_{\min} \text{NEP}, \quad (\text{C-3})$$

where $(S/N)_{\min}$ is the S/N ratio required for detection, and NEP is the noise equivalent power, which is the incident power that produces a signal equal to

*George Lewis is Associate Director of the Security Studies Program at Massachusetts Institute of Technology.

the average noise signal (that is, the NEP is the incident signal power that gives a signal-to-noise ratio of one).

Sensitivity of THAAD Seeker

Detectors are generally characterized by their specific detectivity D^* , which is related to the NEP by the following relation:

$$\text{NEP} = (A_d \times B)^{1/2} / D^*, \quad (\text{C-4})$$

where A_d is the area of a detector element, and B is the bandwidth. D^* is generally given in units of $\text{cm}\cdot\text{Hz}^{1/2}\cdot\text{W}^{-1}$, referred to as a Jones. Next we estimate D^* for a THAAD-like seeker.

The THAAD seeker will use an InSB array.⁶⁵ InSb is sensitive over the range from about $2 \mu\text{m}$ to its cutoff at about $5.6 \mu\text{m}$.⁶⁶ The array must be cooled to at least 80 K. As of the mid-1990s, arrays as large as 256×256 were commercially available. Quantum efficiencies of close to 0.9 are possible.

Several data sheets on InSb arrays give as D^* values (in general D^* rises rapidly as the temperature is reduced below 80K):⁶⁷

4×10^{11} at 77 K and 5×10^{12} at 60 K;

1 to 2×10^{12} at 74 K;

4.2×10^{11} (from 60 to 90 K); and

3.7×10^{12} at 77 K.

These values indicate that, as of the mid-1990s, D^* values of roughly 1 to 5×10^{12} can be achieved with commercially available arrays, assuming the array can be cooled to 77 K or somewhat below.

However, these D^* figures are for detectors which are limited by internal detector noise, which may not be the case for the THAAD seeker, which looks out through an uncooled window. These figures would apply, for example, for a cooled seeker system observing a cold space background through a cooled window (or with no window at all). However, in situations in which a detector looks upon a warm background (such as the earth), or through an uncooled window at a cold background, noise in the background signal may be larger than the internal detector noise. In this case, a different value of D^* may apply (known as the background limited D^* or D_{BLIP}^*).

For our situation, D_{BLIP}^* can be calculated using the following equation:⁶⁸

$$D_{\text{BLIP}}^* = \frac{\lambda_c}{2hc} \cdot \left(\frac{\eta}{\pi c} \right)^{\frac{1}{2}} \cdot \left[\int_{\lambda_1}^{\lambda_c} \frac{\varepsilon}{\lambda^4 (e^{\frac{c_2}{\lambda T}} - 1)} d\lambda \right]^{-\frac{1}{2}} \cdot \left(\sin \frac{\theta}{2} \right)^{-1} \quad (\text{C-5})$$

This equation assumes that the detector is looking at a cold space background through an exterior window of emissivity ε at temperature T . A cooled filter that transmits wavelengths between λ_1 and λ_c is behind the window, and the field of view is limited by a cooled enclosure to a half-angle $\theta/2$. The detector quantum efficiency is given by η , and $c_2 = hc/k$.

The THAAD seeker uses a sapphire window. Since the emissivity is equal to the absorptance, $\varepsilon = 1 - \rho - \tau$, where ρ is the reflection coefficient (reflectance) and τ the transmission coefficient (transmittance). A 2.6 mm thick sapphire window has a transmittance above 0.9 for wavelengths shorter than about 4 μm .⁶⁹ At longer wavelengths, τ falls off rapidly, reaching 0.7 at 5 μm and about 0.5 at 5.6 μm . If a thinner window could be used (for example 0.5 mm), τ could be kept above 0.8 at 5.6 μm .

Since the radiation from a 300 K blackbody peaks at a wavelength of about 12 μm , it is desirable to use a wavelength as close to 12 μm as possible. However, as discussed above, InSb at 77 K can detect wavelengths only below 5.6 μm , and the rapidly falling transmittance of sapphire above 5.0 μm makes it undesirable to use wavelengths longer than 5.0 μm unless a very thin window is used.

Thus here we assume that a cooled filter is used that transmits only between 4.0 and 5.0 μm , and that the average transmittance over this spectral band is $\tau = 0.8$. In this spectral range, the reflection coefficient is about 0.06–0.09.⁷⁰ This gives an emissivity ε of about 0.11–0.14. If we assume that two mirrors are used in the optics and each contributes an emissivity of 0.03, we get an emissivity of roughly 0.20 and so here we take $\varepsilon = 0.20$. We assume that the window is at 300 K.

In order to cut down the noise power on the detector, it is desirable to use cooled shielding to reduce the field of view of the detector down to as low a value as possible. As noted in the main article, a field of view of 1 degree is a reasonable assumption. Here we use a larger value of 3 degrees (that is, a 1.5 degree half angle) for the opening in the cooled shield.

As discussed above, quantum efficiencies of nearly 0.9 can be achieved for InSb. Here we assume only $\eta = 0.6$.

Using $\eta = 0.6$, $\varepsilon = 0.20$, $T = 300$ K, $\theta = 3.0$ degrees, and assuming the cooled filter transmits from 4.0 to 5.0 μm , we get: $D^* = 2.2 \times 10^{13}$ cm-Hz^{-1/2}-W⁻¹.

This result indicates that the detector is not background limited, but is limited by internal detector noise. Noting from detector data sheets that a space-qualified 256×256 InSb array with a D^* of 3.7×10^{12} at $4.6 \mu\text{m}$ was commercially available in the mid-1990s, we use this value for D^* .⁷¹

Detection Range

We next estimate the detection range against a relatively small strategic target. The MK-12A reentry vehicle used on U.S. Minuteman missiles has a base diameter of 54.3 cm and a length less than 181.3 cm.⁷² Using these dimensions, the warhead would have a surface area of about 1.8 m^2 . If the target is at 300 K and has an emissivity of 0.9, then in the band from 4.0 to $5.0 \mu\text{m}$, from Equation (C-1) it would emit $4.6 \times 10^{-4} \text{ W/cm}^2$, for a total of $\Phi_T = 8.3 \text{ W}$.

The noise equivalent power for the detector is then given by:

$$\text{NEP} = (A_d \times B)^{1/2} / D^*. \quad (\text{C-6})$$

Detector data sheets indicate that typical detector spacings for 256×256 arrays are about 30–40 μm . Thus we take the detector size to be 35 μm . Assuming a bandwidth of 50 Hz (that is 50 detector measurements per second), we get: $\text{NEP} = 6.6 \times 10^{-15} \text{ W}$.

A S/N of 13.6 dB (= 22.9) gives a 90% single-look probability of detection with a false alarm probability of 10^{-7} .⁷³ A total power of $\Phi_D = 1.5 \times 10^{-13} \text{ W}$ is then required for detection. Assuming system losses equal to 20% ($L = 1.2$) and a 10 cm diameter optical aperture, then the detection range R is given by:

$$R^2 = \Phi_T A / 4\pi \Phi_D L \quad (\text{C-7})$$

which gives $R = 170 \text{ km}$.

This is a detection range averaged over the reentry vehicle's orientation. For an unfavorable viewing orientation, such as nose-on or base-on, the signal is reduced by a factor of about 2, giving a minimum detection range of about 120 km.⁷⁴ Detection ranges at different temperatures are shown in Figure C-1, based on a detection range of 120 km at 300 K.

Thus a minimum detection range of at least 120 km against a small strategic target seems reasonable. This number is of course not only just a rough estimate, but is also somewhat arbitrary, because it depends on the requirements set on the detection probability, the false-alarm rate, and other assumptions. Greater detection ranges could be obtained by relaxing these requirements

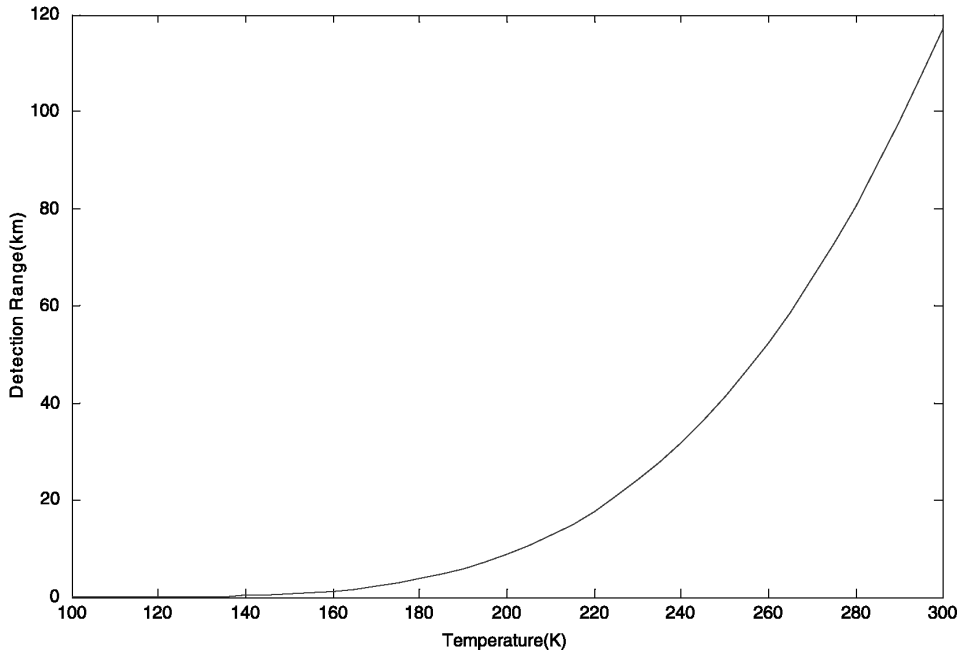


Figure C-1: THAAD-like KV's detection range at different target temperatures.

somewhat. Significantly greater detection ranges would also be possible against larger RV targets. On the other hand, if the detector noise limited value of D^* is smaller than 3.7×10^{12} value used here, the detection range will be decreased (the detection range will decrease as the square root of D^*).